Diagnostics for shock ignition

Dimitri Batani

National Research Nuclear University MEPhI

University of Bordeaux

X Conference on "Modern Techniques of Plasma Diagnosis and their Application" 14 – 16 November, 2016 at National Research Nuclear University MEPhI

10-я конференция

"Современные средства диагностики плазмы и их применение"

Москва, НИЯУ МИФИ, 14-16 ноября 2016 г.

16 НОЯБРЯ 2016 г.

Direct Drive ICF

We need DIRECT DRIVE for future reactors

- Higher gains
- Smaller laser facilities
- Simpler targets and simpler scheme more compatible with high-repetition rate operation and requirements of fusion reactors

Unfortunately Direct Drive is prone to uniformity problems and hydro-instabilities (Rayleigh-Taylor)

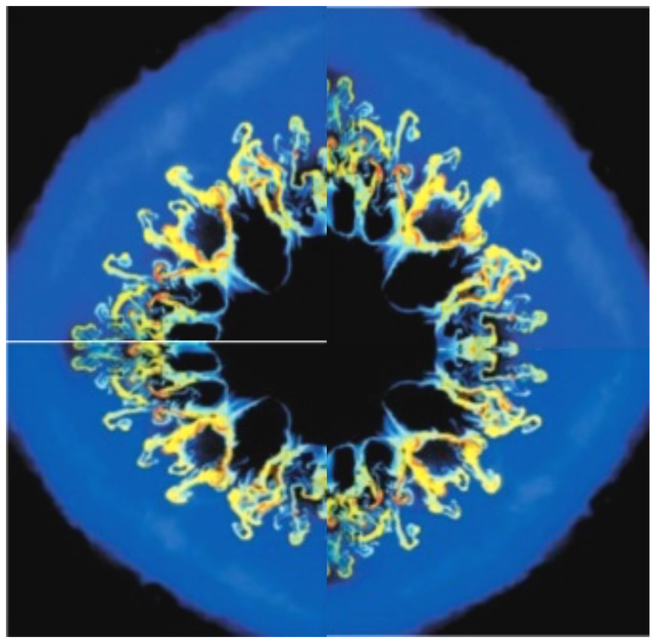

Possible Solution:

Decoupling compression and ignition

➔ Fast Ignition

➔ Shock Ignition

Shock Ignition

Low velocity driveV~240 km/s
Low AR

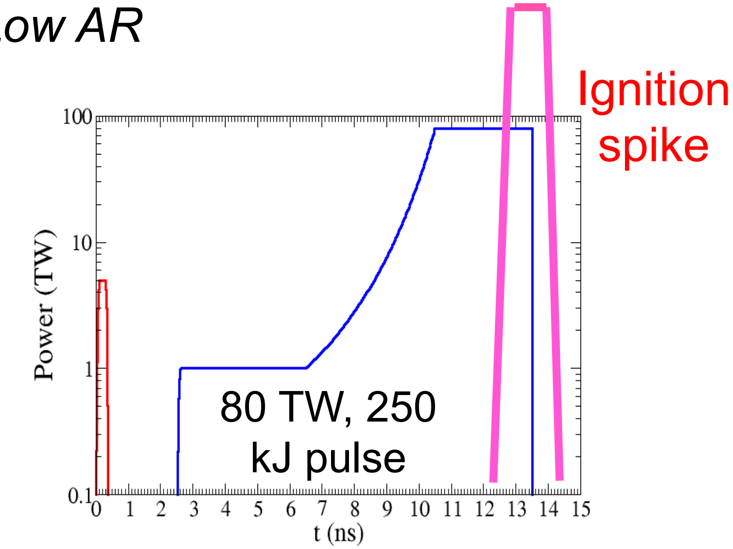

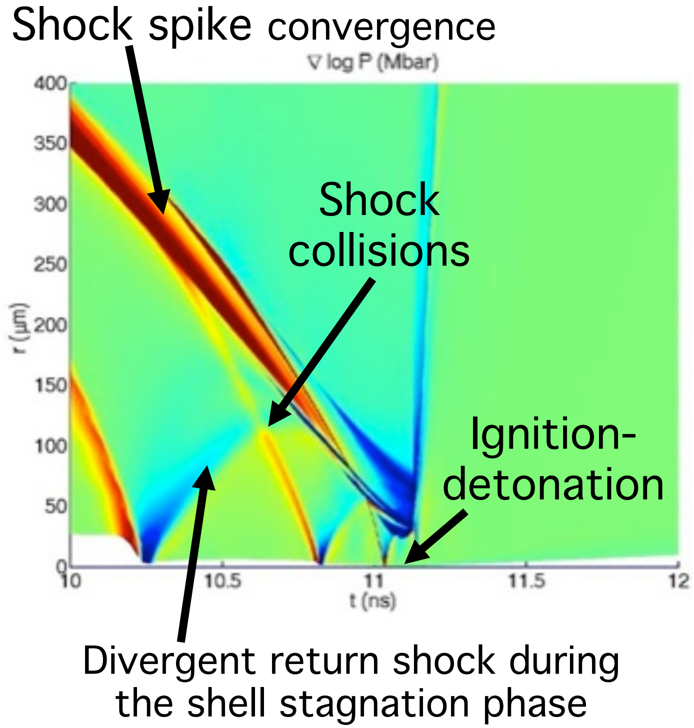

- *Scheme proposed by by R. Betti, J.Perkins et al. [PRL 98 (2007)] and anticipated by V. A. Shcherbakov [Sov. J. Plasma Phys. 9(2) 240 (1983)]*
- A final laser spike launches a converging shock
- The ignition shock collides with the return shock resulting in shock amplification and providing conditions for triggering ignition from central hot spot
- RESULTS IN A NON-ISOBARIC FUEL ASSEMBLY

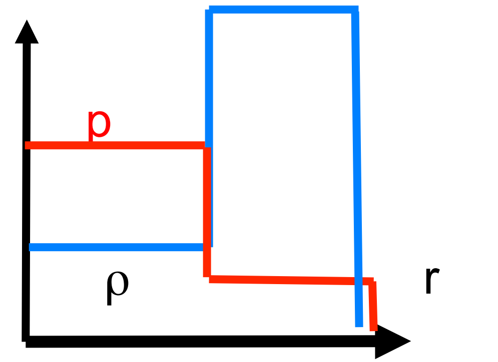

Fuel assembly is non isobaric

Advantages of Shock Ignition

1) The compression phase does not need to provide a central hot spot; we can implode a thicker target (low AR) at lower velocity, much less sensitive to hydro instabilities

2) Non isobaric fuel assembly implies higher gains

HiPER target at ignition time

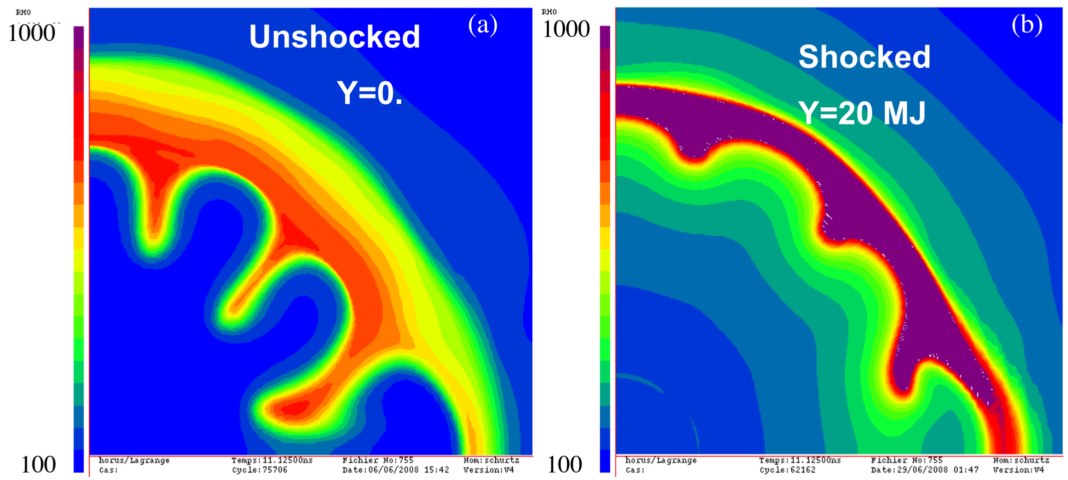

In addition RT growth can also be mitigated due to:

- Strong radiation emission from hot plasma produced at shock convergence (mitigates RT growth at stagnation)

- Competition between Rayleigh-Taylor and Ritchmayer-Meskhov

Unknowns of Shock Ignition

- Effect of laser-plasma instabilities at intensities up to ≈ 10^{16} W/cm^2. SRS, SBS and TPD. How they develop? How much light do they reflect?

- Hot electrons number and energy? What is their effect? *(usually in ICF hot electrons preheat the target and are dangerous ... Here they came at late times, large fuel ρr, so they could indeed be not harmful or even beneficial, increasing laser-target coupling in presence of a very extended plasma corona...)*

- Are we really able to couple the high-intensity laser beam to the payload through an extended plasma corona? Are we able to create a strong shock?

- What is the effect of magnetic fields, delocalised transport, delocalised absorption, thermal smoothing in the overdense region on shock generation at high laser intensity?

Diagnostics for Shock Ignition

- A variety of diagnostics is needed to allow detecting the complex physics involved in shock ignition
- Diagnostics for shock dynamics (SOP, VISAR, X-ray radiography)
- Diagnostics for hot electrons
- Diagnostics for the onset of parametric instabilities

Etc. etc.

Experiments in planar geometry allow unrevealing much of the physics of shock ignition. Experiments have been done in European Laser Facilities like PALS, LULI, LIL, etc..

See review paper: D.Batani, S.Baton, A.Casner, S.Depierreux, M.Hohenberger, O.Klimo, M.Koenig, C.Labaune, X.Ribeyre, C.Rousseaux, G.Schurtz, W.Theobald, V.Tikhonchuk «Physical issues in shock ignition» Nuclear Fusion, 54, 054009 (2014)

Diagnostics for Shock Dynamics

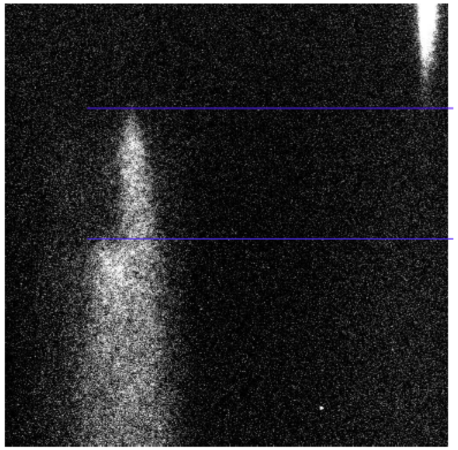

Shock chronometry
(SOP: Streaked Optical Pyrometry)

VISAR (Velocity Interferometer System for Any Reflector)

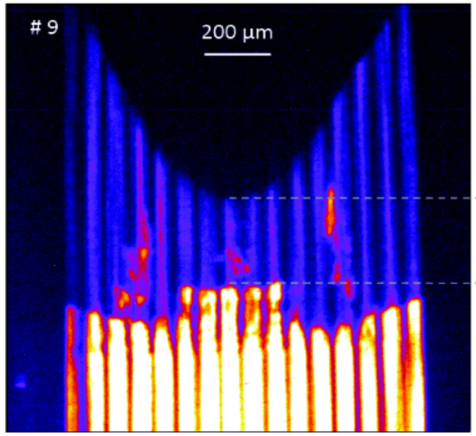

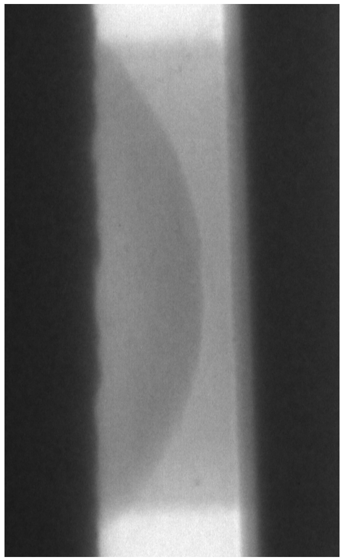

Time resolved X-ray radiography
(1D or 2D)

Experiments at PALS - Prague

The PALS Iodine Laser
λ =1.3 μm
τ = 300 ps
3ω λ =0.44 μm
E ≤ 500 J

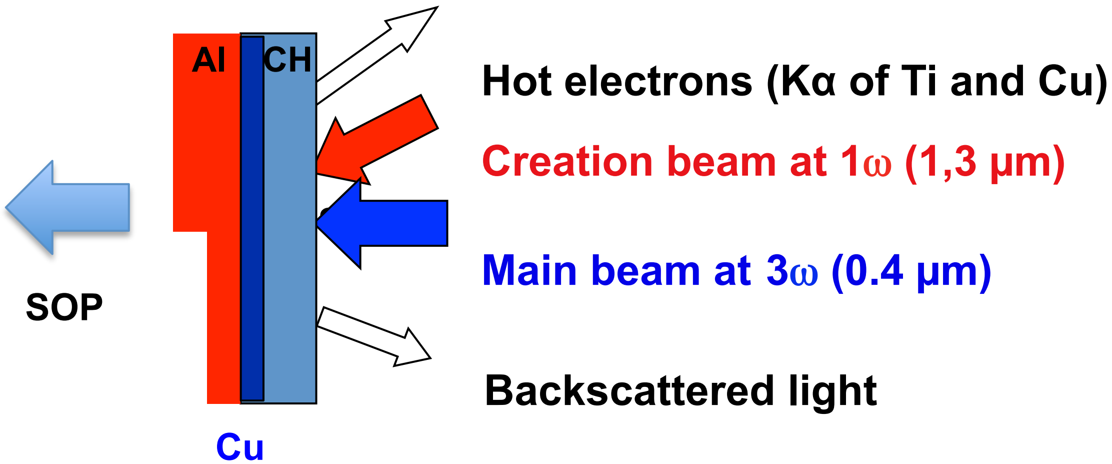

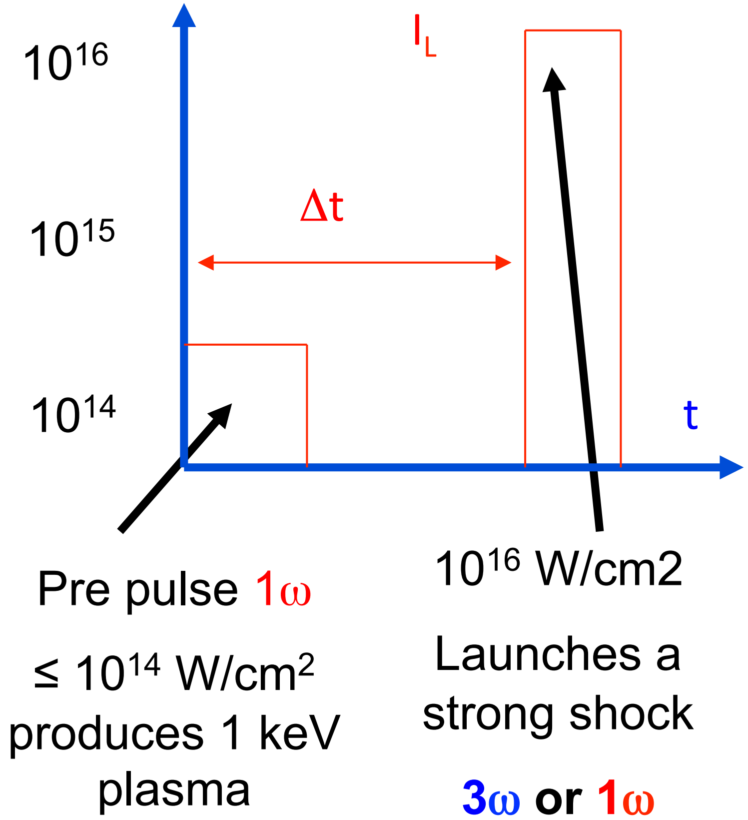

D. Batani, et al. "Generation of High Pressure Shocks relevant to the Shock-Ignition Intensity Regime" Physics of Plasmas, **21**, 032710 (2014)

Shock chronometry

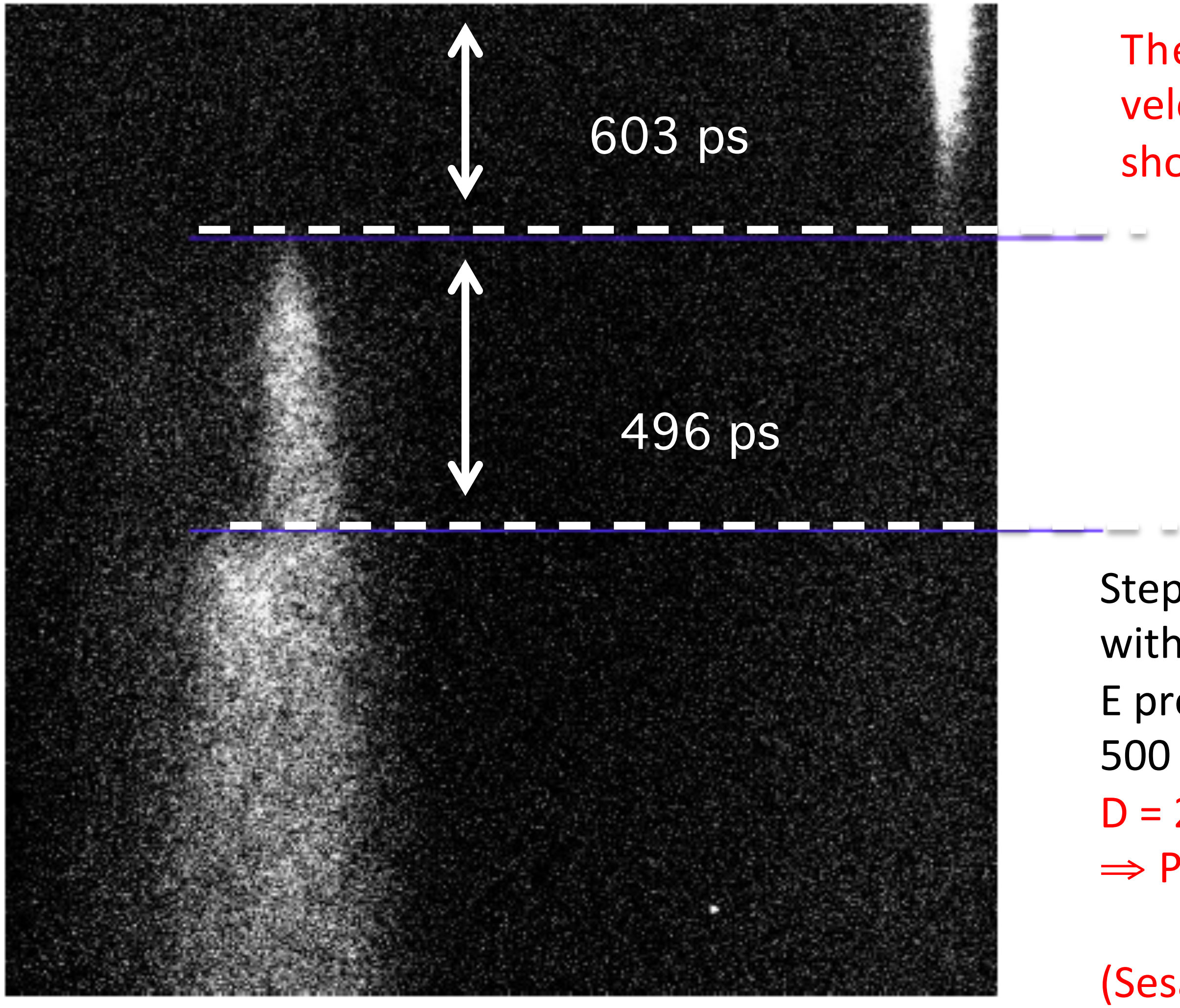

The measurement of shock velocity provides the value of shock pressure using an EOS

Stepped target (10 µm Al)
with E(3ω) = 245 J
E pre-pulse = 29 J, delay prepulse 500 ps
D = 20.2 km/s
⇒ P = 6.3 Mbar

(Sesame Tables for Al)

Shock chronometry for estimating the pressure

Measured P at rear side much lower than ablation pressure at front side:
Shock pressure undergoes a rapid decrease due to:
1) 2D effects during propagation
2) Relaxation waves from front side when laser turns off

Target
25 μm CH
35 μm Al

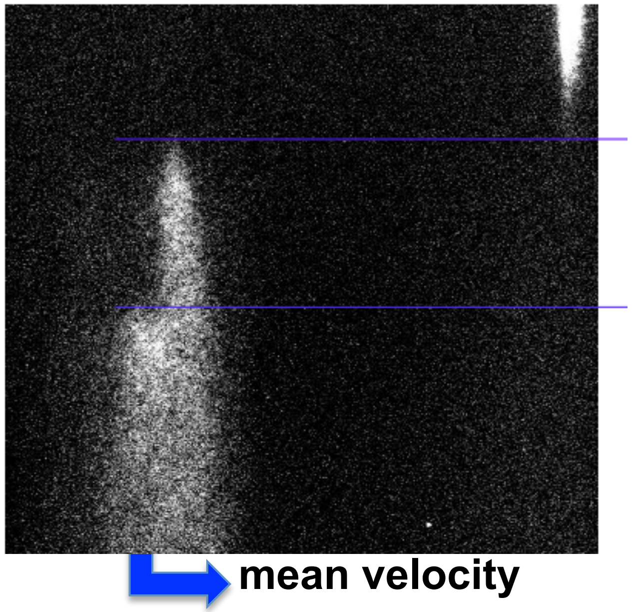

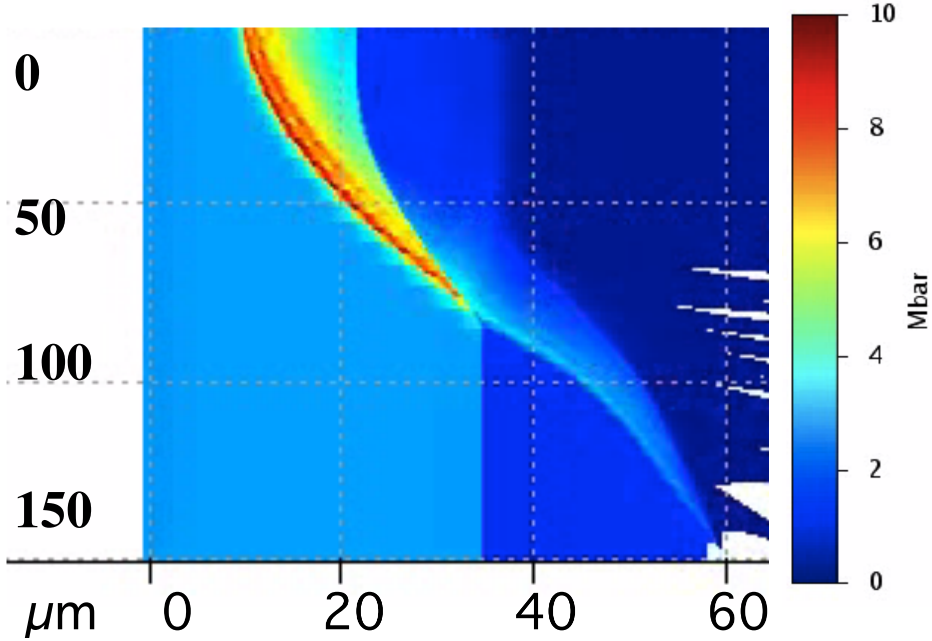

We run hydro simulations to match shock breakout time and find that a final pressure ≤ 10 Mbar corresponds to P ≈ 90 Mbar during interaction

Due to impedance mismatch, it increases to 130 Mbar for Al and 210 Mbar for Cu.

2D Hydro simulations

Initial ablation pressure ≈ 90 Mbar

Still << estimation from scaling laws

$P \approx (\eta\, I / \lambda)^{2/3}$

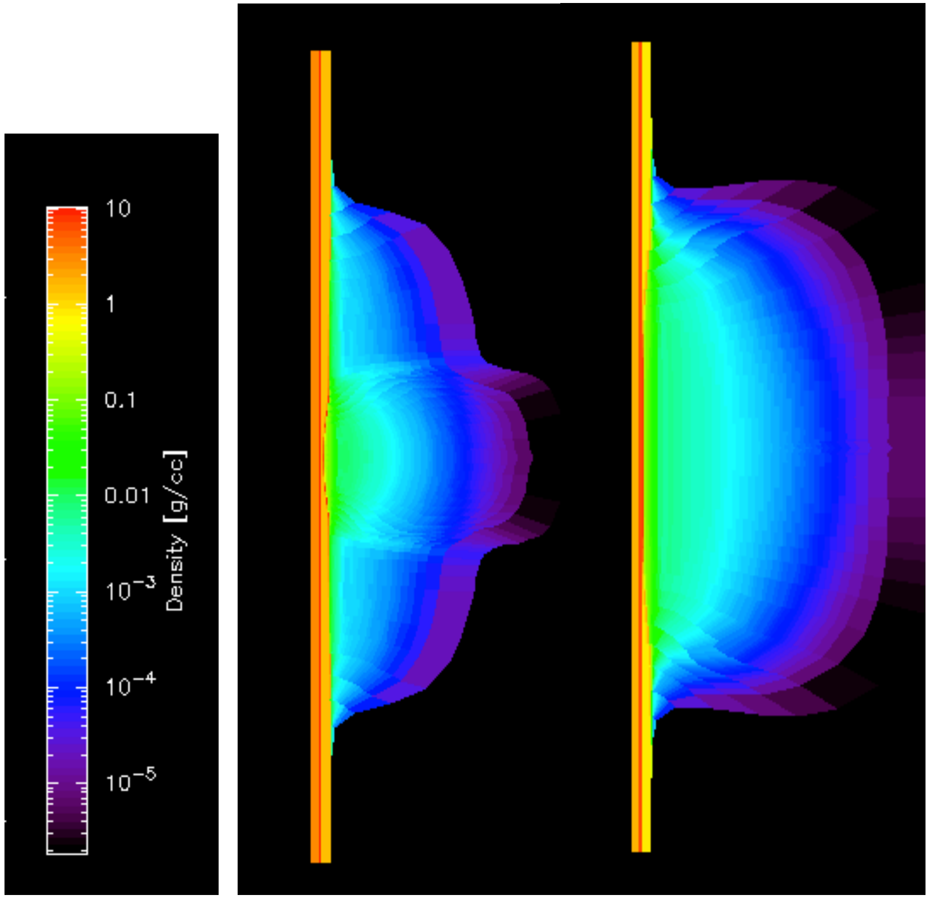

Explanations ?

Lateral energy transport in the overdense region due to the distance between absorption region and ablation front In our experiment the spot size is comparable to the distance between critical layer and ablation surface (≈40 µm vs. ≈100 µm)

Simulations with the same laser parameters but larger spot (≥ 400 µm) yield pressure ≈ 180 Mbar

***Lateral heat transport* in the *overdense region* is important and reduces the shock pressure**

Simulated SOP images

changing hot electron temperature and energy conversion electron beam

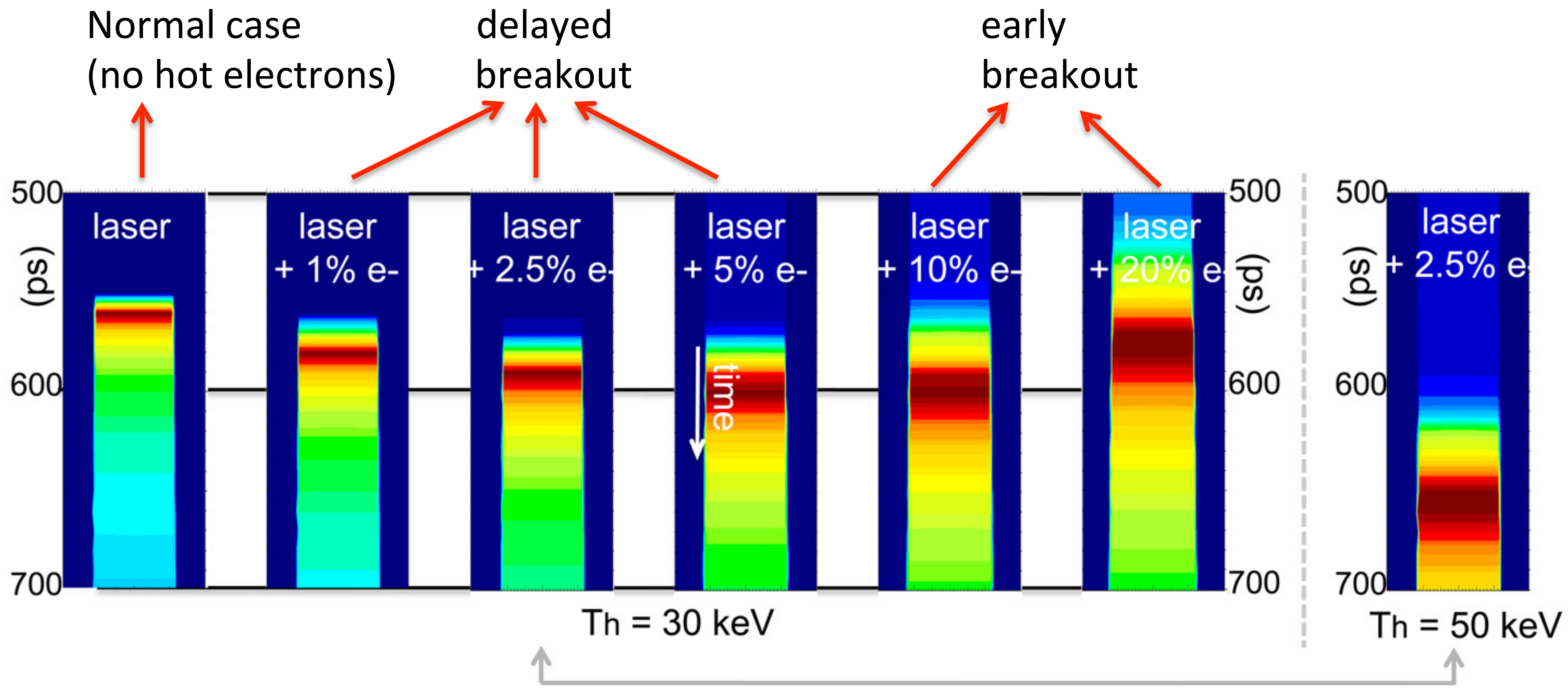

"Effect of nonthermal electrons on the shock formation in a laser driven plasma" Ph.Nicolaï et al. Phys. Plasmas, 22, 042705 (2015)

“Improved” CHIC simulation code

- Better description of absorption (from ray tracing to “thick” gaussian beamlets) [A.Colaïtis et al., PRE (2013)]
- Possibility of superimposing many beamlets reproducing the speckle structure of a realistic focal spot
- Real time treatment of parametric instabilities and resonant absorption. Calculation of back-reflected light and generation of hot electrons (using published scaling laws)
- Hot electrons coupling to hydro (using a reduced fast kinetic “M1” transport model [M.Touati, et al., New J. Phys. 16, 073014, 2014)]

A. Colaïtis, et al. «Coupled hydrodynamic model for laser-plasma interaction and hot electron generation» PRE 92, 041101(R) (2015)

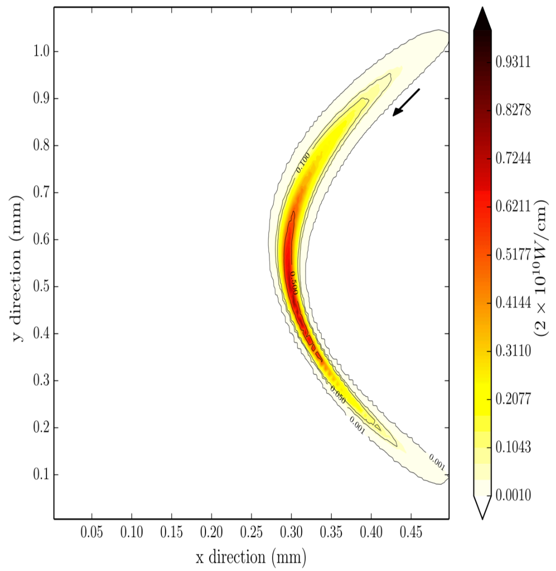

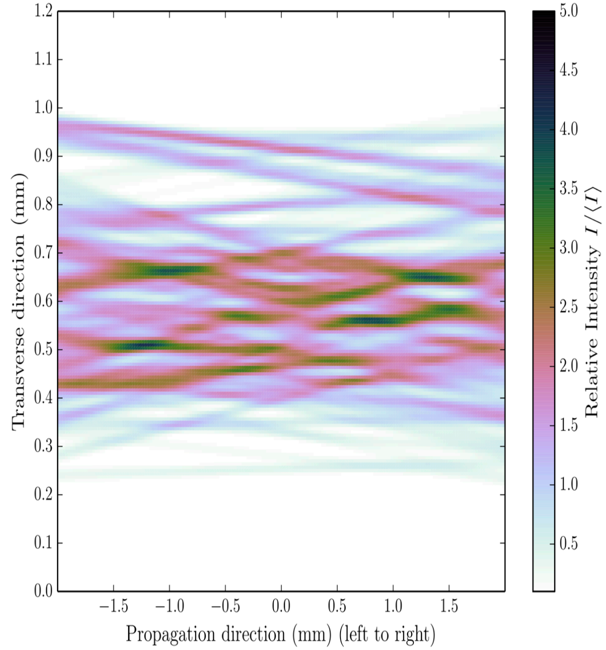

Simulations with "improved" model

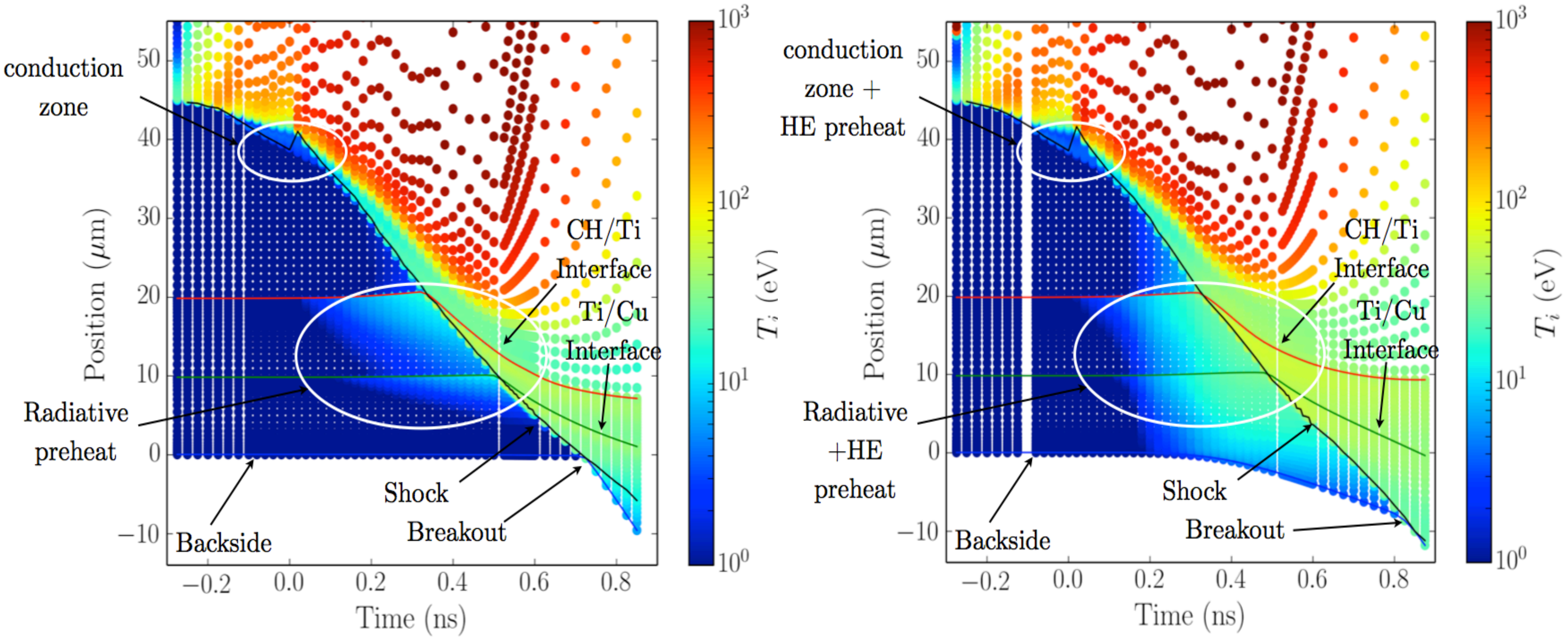

CH/Ti/Cu target **Without hot electrons** **With hot electrons**

Hot electrons preheat the target which expands resulting in delayed shock breakout

Shock velocity increases as $\rho^{-1/2}$
But crossed thickness increases as ρ^{-1}

Experiments at LIL and LULI

- LIL is the prototype of laser Megajoule LMJ
- Irradiation at 3ω in long pulse (2 ns) up to 15 kJ
- Random Phase Plates for Gaussian Focal spot
- Laser intensity up to 4 10^{15} W/cm^2

CELIA

Experiment at LIL (and LULI)

Main interest: LIL allows reproducing plasma scale-lengths typical of LMJ

Two laser pulses

1. wo pre-plasma

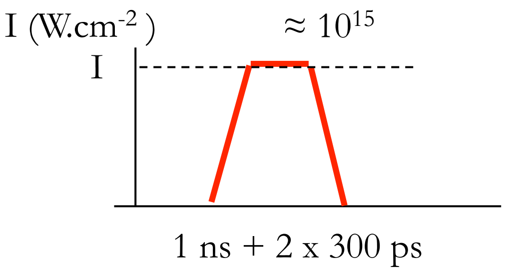

2. with pre-plasma

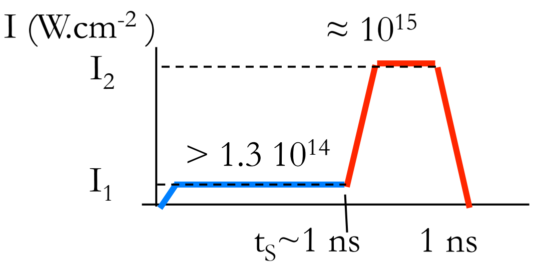

Two target geometries

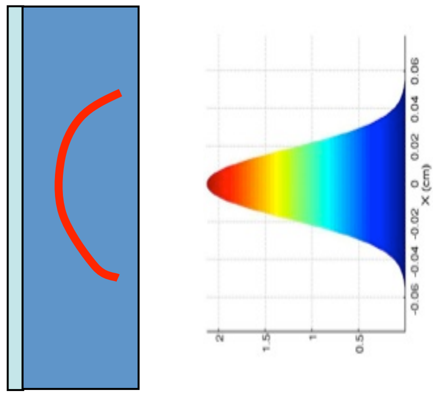

Planar target:
Divergent shock
Lateral losses

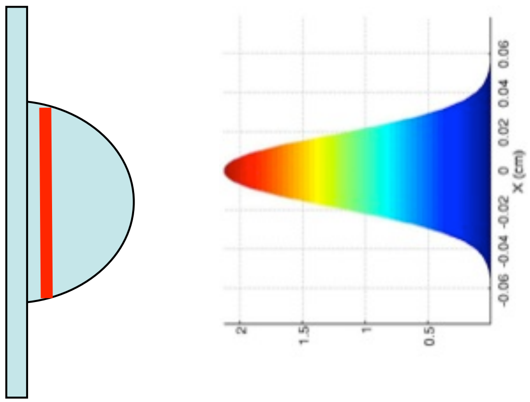

Hemispherical target:
Planar shock
Reduced losses

1) Influence of preplasma
2) «Spherical effects» in plane geometry (e.g. absorption at oblique incidence) ➔ PPD
3) «Flatten» the shock (better measurements based on X-ray radiography or VISARs)
4) Smoothing effects (preparing bipolar shock wave experiments)

Velocity from expt data

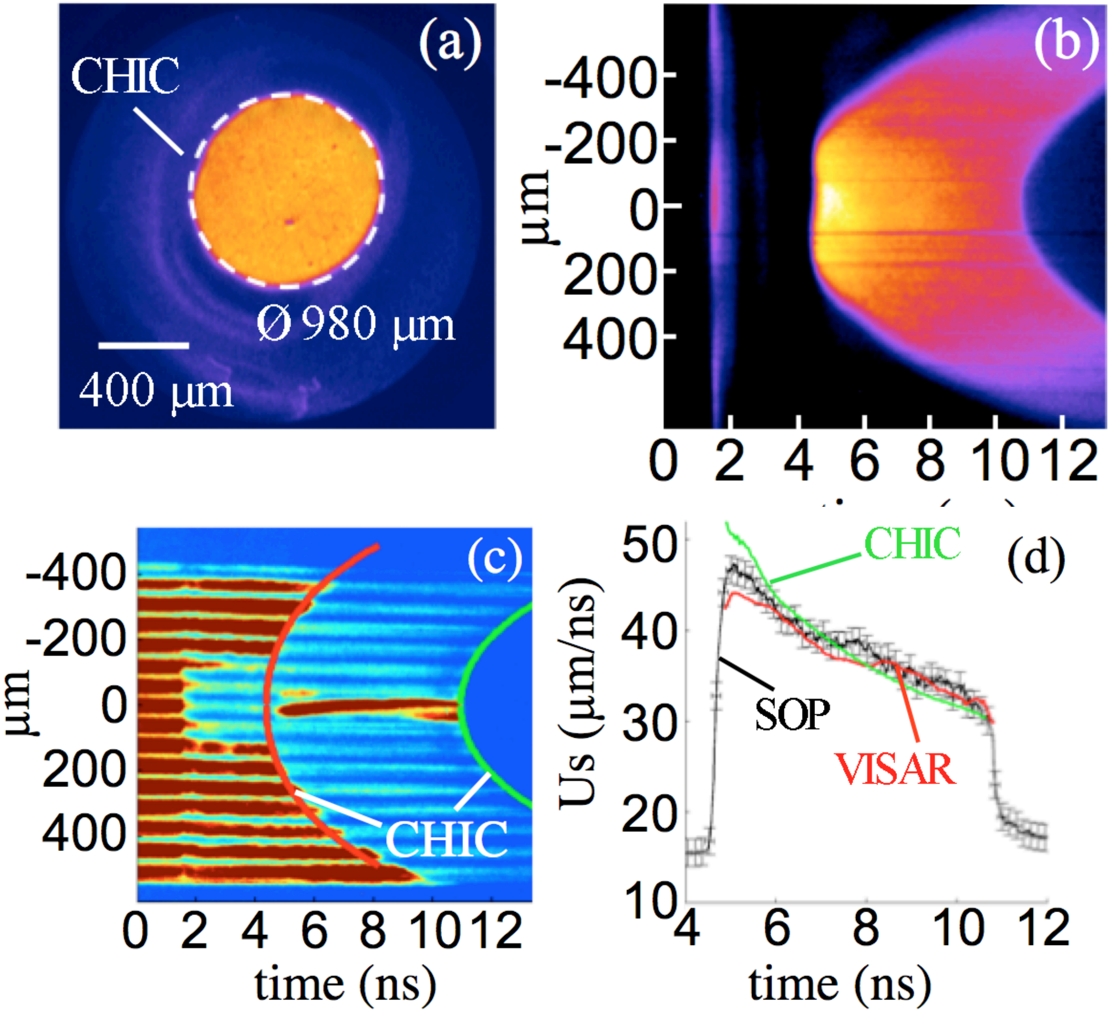

Experimental shock propagation data obtained with (a) GOI, (b) SOP and (c) VISAR with a planar target. (d) shows extracted shock velocities from VISAR and SOP and calculated from CHIC

An accurate absolute calibration of the SOP and an accurate knowledge of quartz equation of state allowsr retrieving the shock velocity from SOP data

Examples of results (VISAR)

$E_{LULI2000}(2\omega) = 400$ J

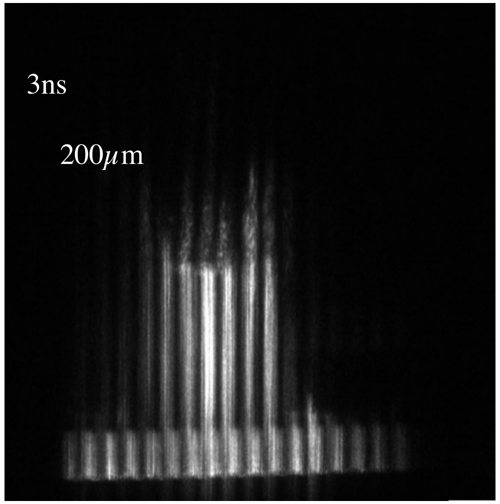

LULI

$E_{LIL}(3\omega) = 9700$ J

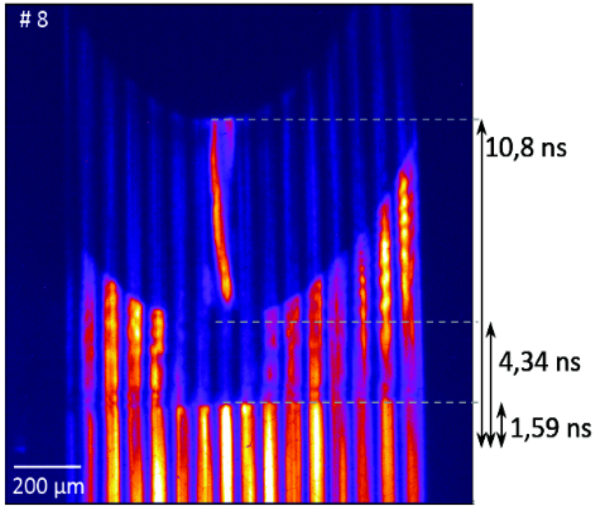

LIL

$E_{LIL}(3\omega) = 9900$ J

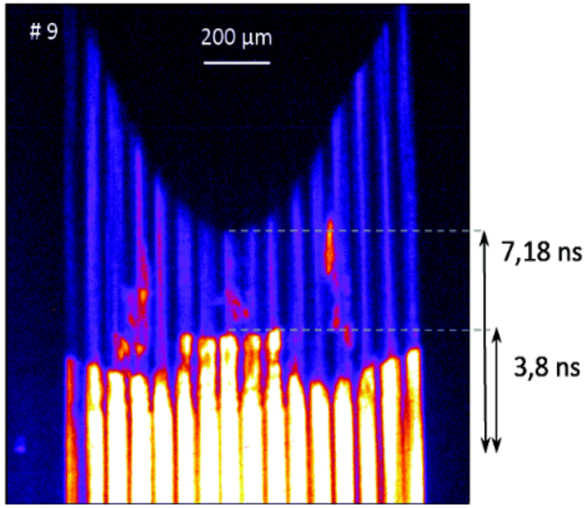

LIL

CH Cylinder
250 µm thick

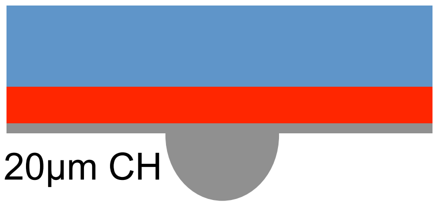

Quartz
250µm

15µm
Mo

20µm CH

CH Hemisphere
500 µm diameter

AR @532nm on rear side

Examples of results (VISAR)

$E_{LULI2000}(2\omega) = 400$ J

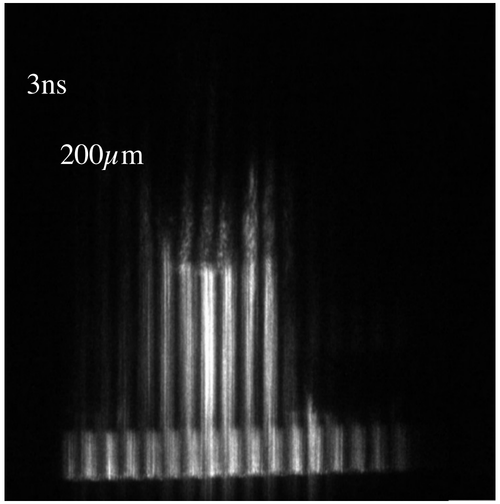

LULI

$E_{LIL}(3\omega) = 9700$ J

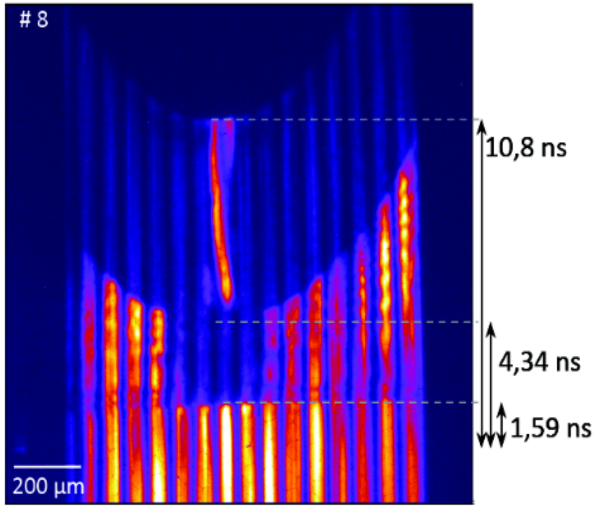

LIL

$E_{LIL}(3\omega) = 9900$ J

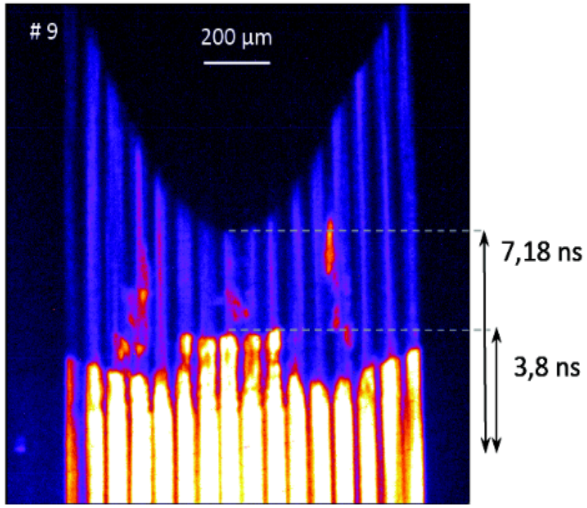

LIL

CH Cylinder
250 µm thick

AR @532nm on rear side

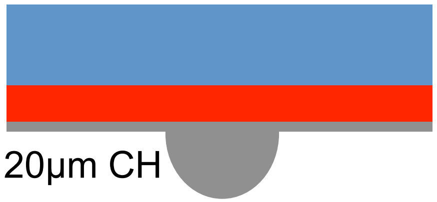

Quartz
250µm

15µm
Mo

20µm CH

CH Hemisphere
500 µm diameter

LIL: spherical shot, with pp

Shot #9 sphere with pre-plasma
EOS T7385 for alpha quartz

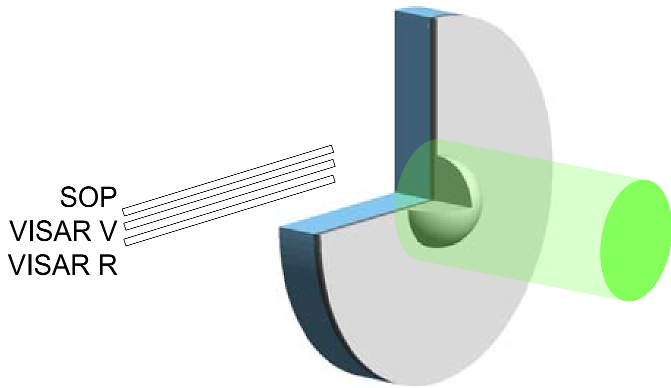

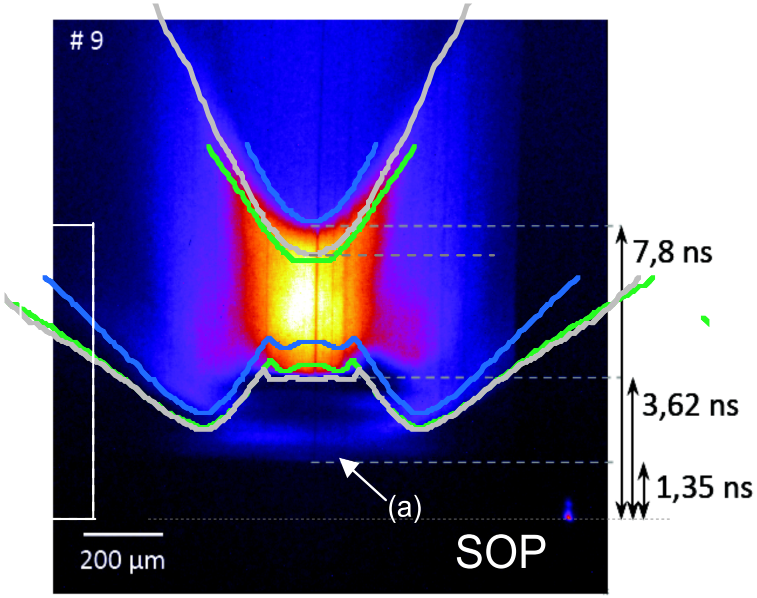

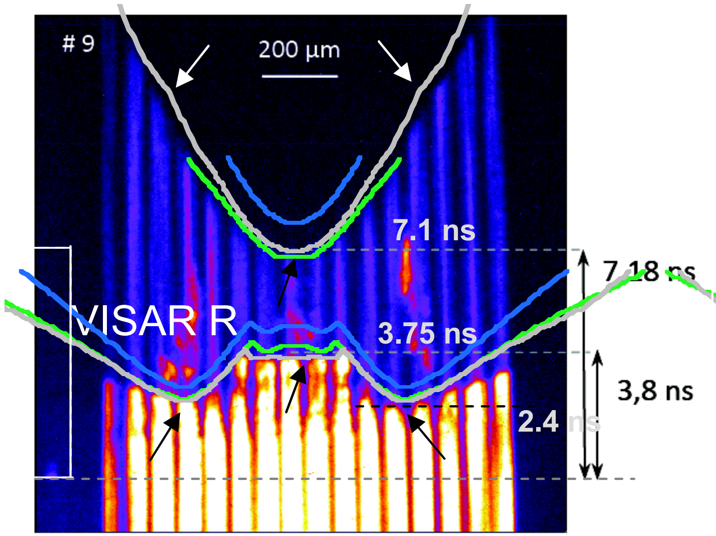

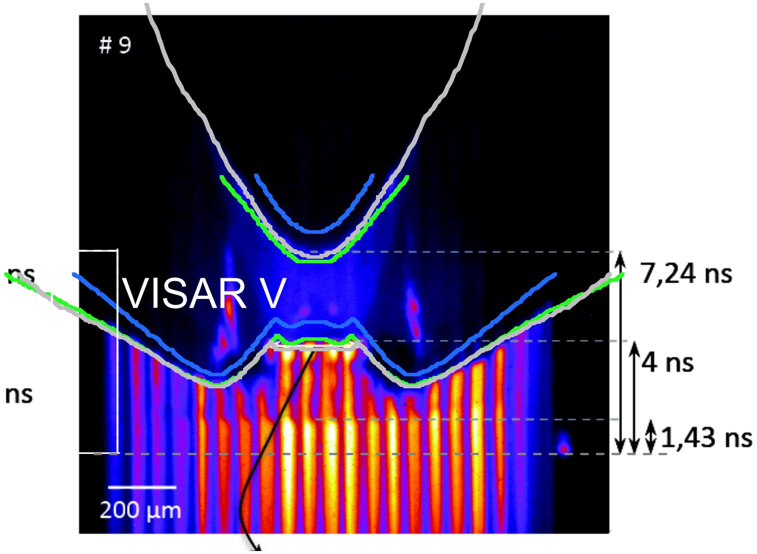

LIL: experimental results

Tir		P_L (W)	I (10^{15}W/cm^2)	P_a (scale law)	P_{2D}
# 8pp*	plan	4.10^{12}	3.0	119	90
# 9pp*	sph	3.9 10^{12}	2.9	117	115
# 10	sph	4.2 10^{12}	3.1	123	120
# 11	plan	4.4 10^{12}	3.2	126	105
# 12	sph	6. 10^{12}	4.4	140 (70% abs)	140

Pressures up to 140 Mbar.

Agreement with scaling laws seems reasonable

Intensities up to 4.4 10^{15} W/cm^2 (but this is the max in space and time in intensity distribution)

Drawbacks of SOP / VISARS

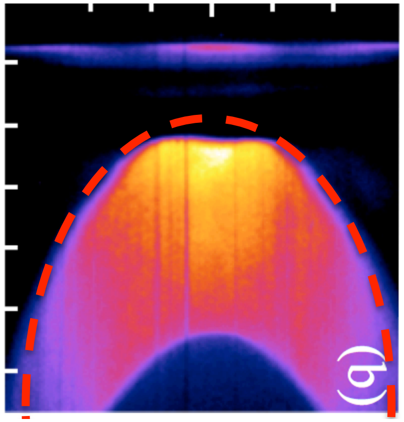

VISAR and SOP become blind at very early time because the intense target preheating make the material (quartz) opaque

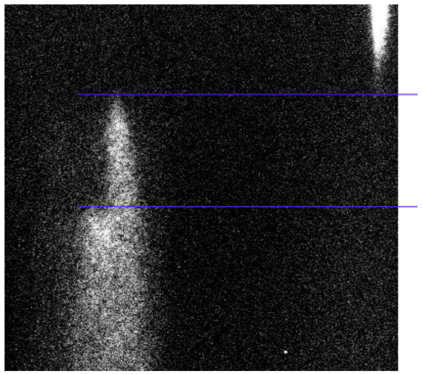

SOP is good for shock chronometry of stepped targets are used without a layer of transparent material (quartz) on the back

In order to overcome this problem we tested the possibility of using time-resolved X-ray radiography as a diagnostics of shock dynamics

2D radiography with ps beam

Experimental set-up (LULI)

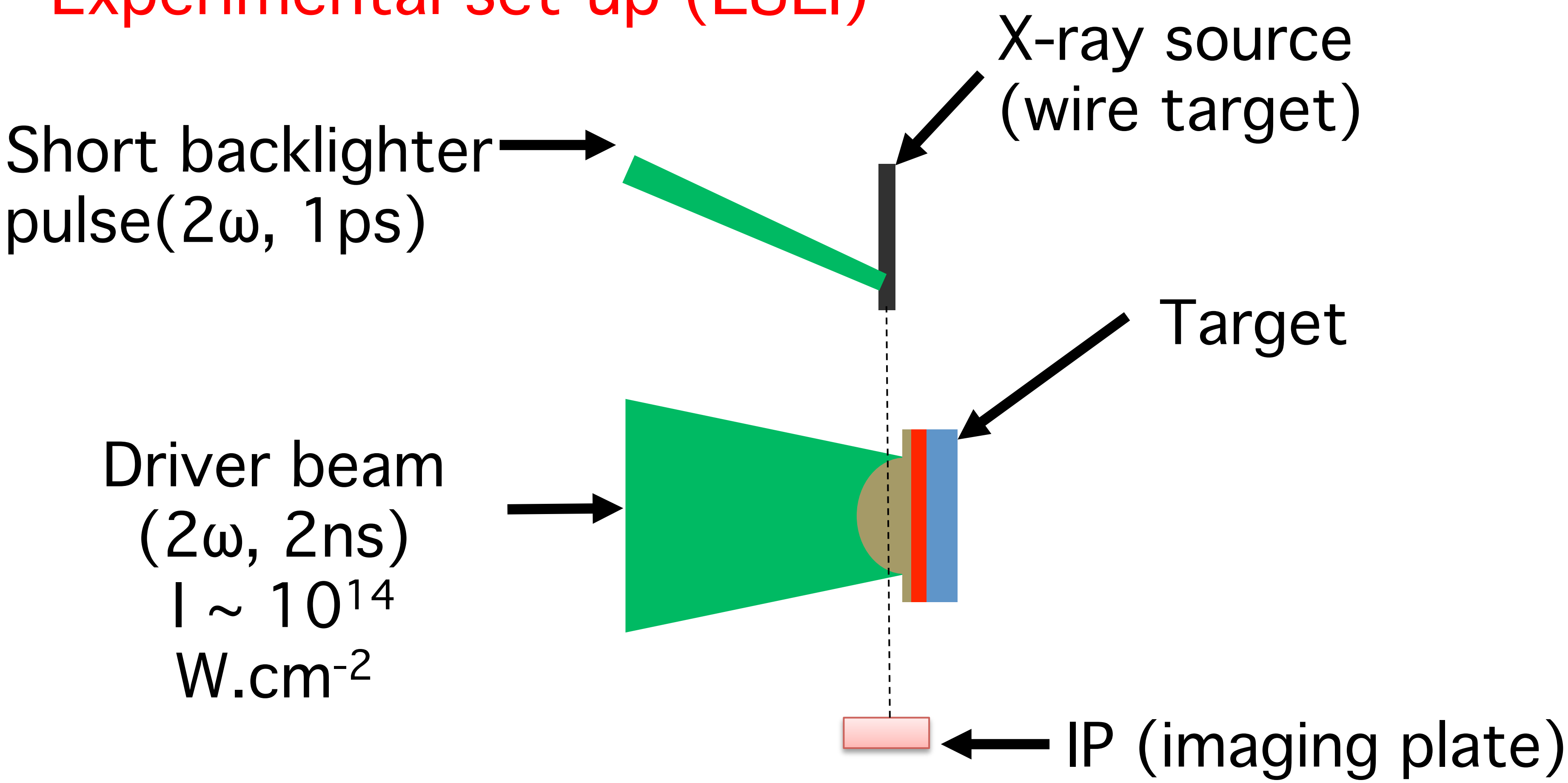

Example of results

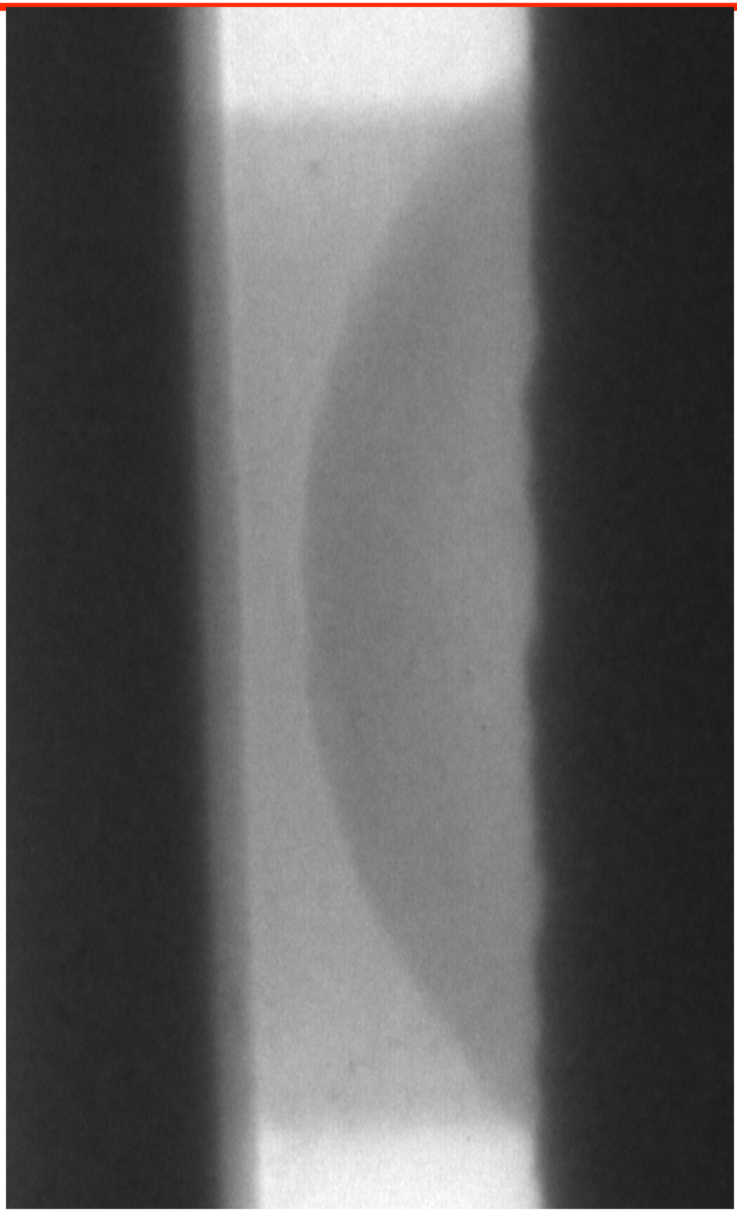

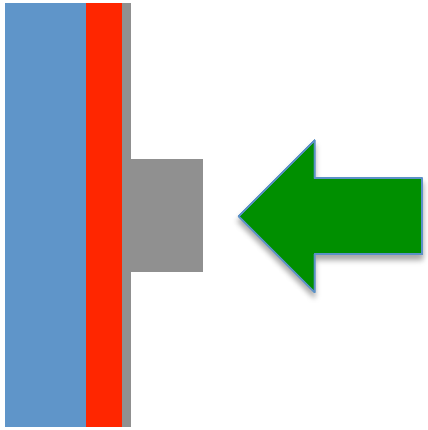

Radiography of a target composed of 250 microns of SiO_2, 15 microns of Mo, 20 microns of CH, a cylinder of 500 microns diameter and 250 of height (laser side). The focal spot was a Gaussian with 400 microns diameter, energy (2ω) = 409J, pulse duration of 2ns. Radiography used K-a emission from a V backlighter target irradiated with a short pulse (1ps) with energy(2ω) = 22J, 4.7ns after the shock creation.

Conventional treatment

Abel inversion

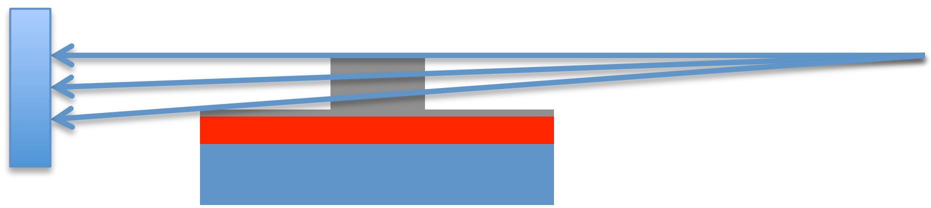

$$I(y,z) = I_0 \exp\left(-\int_{-x_0}^{+x_0} k(E,x,y,z)dx\right) = I_0 \exp\left(-2\int_{0}^{+x_0} k(E,x,y,z)dx\right)$$

$$k(E,x,y) = \mu(E,x,y)\rho(x,y)$$

$$k(E,r,z) = \frac{1}{\pi}\int_{r}^{+\infty} \frac{d}{dx}\left[\ln\left(\frac{I(y,z)}{I_0}\right)\right]\frac{dy}{\sqrt{y^2-r^2}}$$

Problems:

- Very noisy
- Assume parallel beam
- Does not take into account source size

Abel Inversion

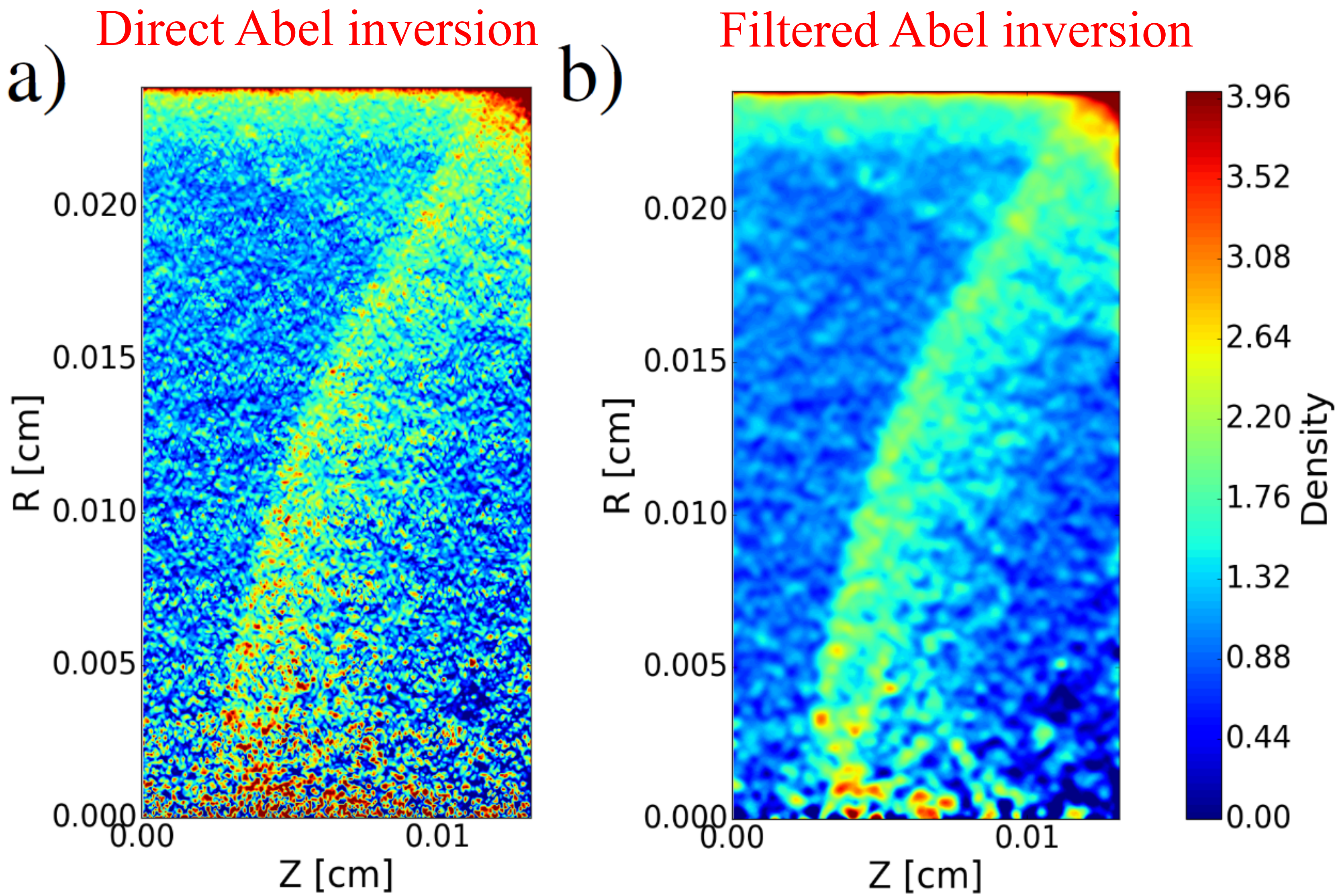

Abel Inversion

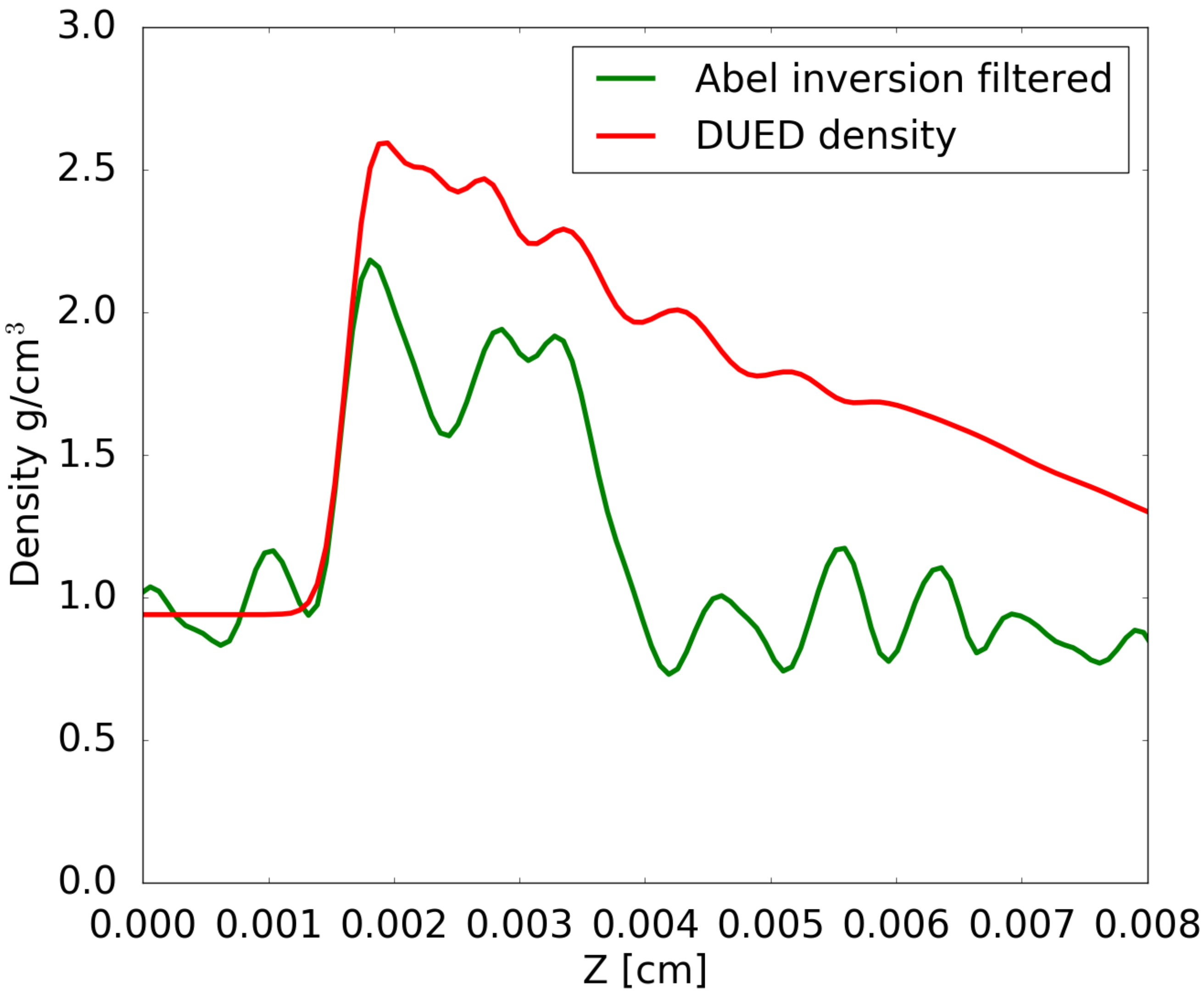

The previously cited problems result in not good reproduction of the density profile (not consistent with hydro simulations and with experimental measurement of shock velocity)

Synthetic radiographies (DUED)

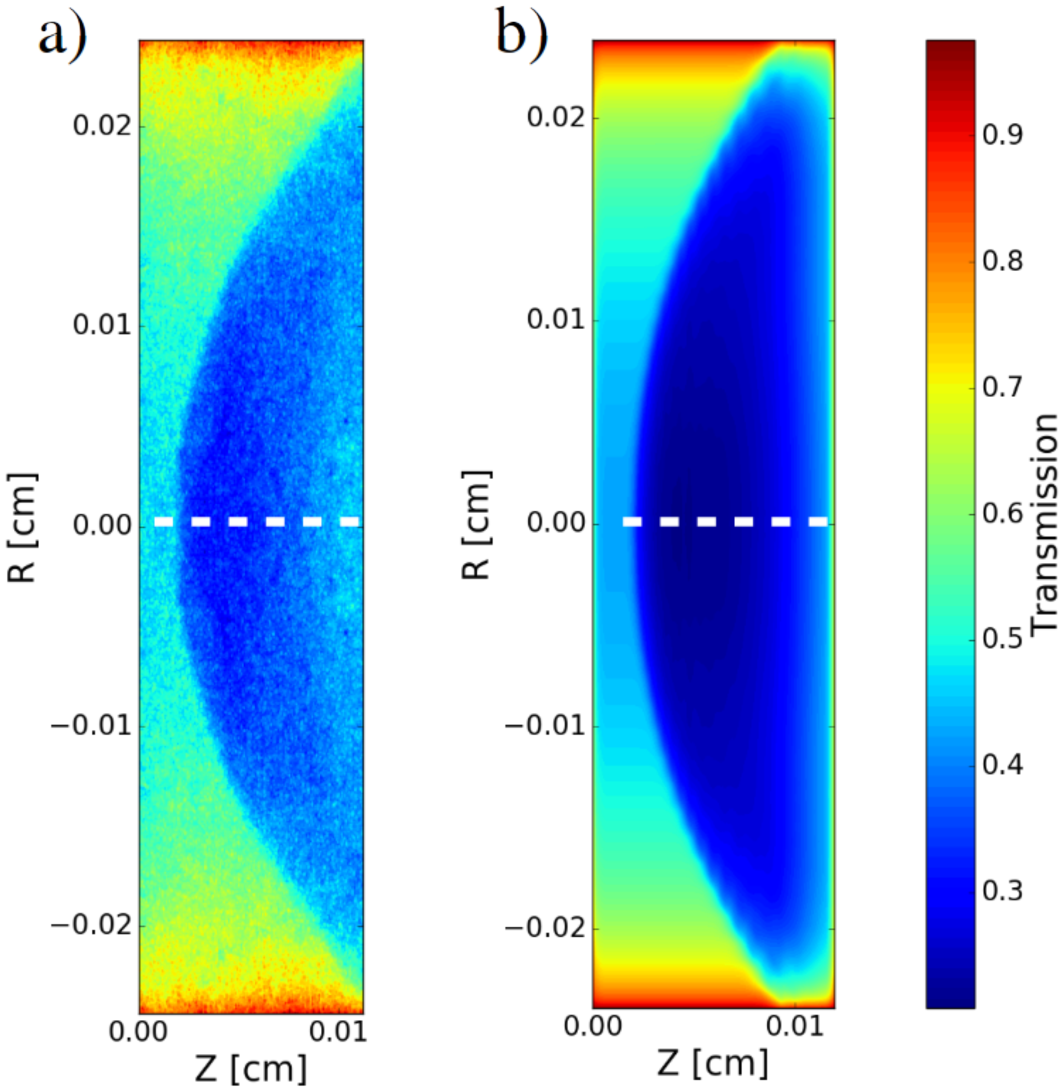

Cylindrical Target

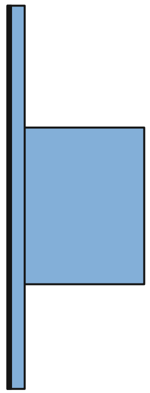

t = 4.7 ns

Synthetic radiographies

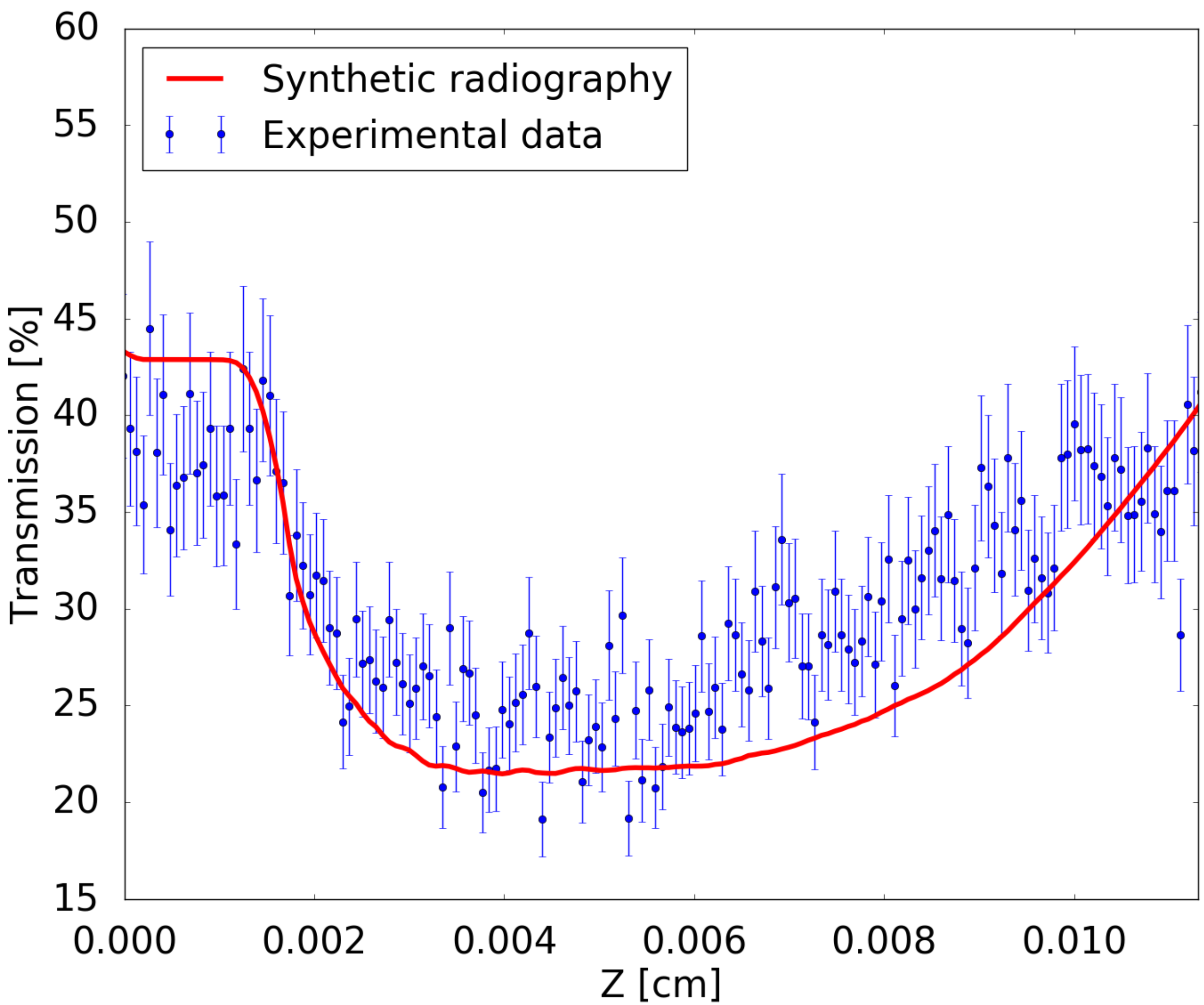

Comparison of measured / predicted transmission

Synthetic radiographies

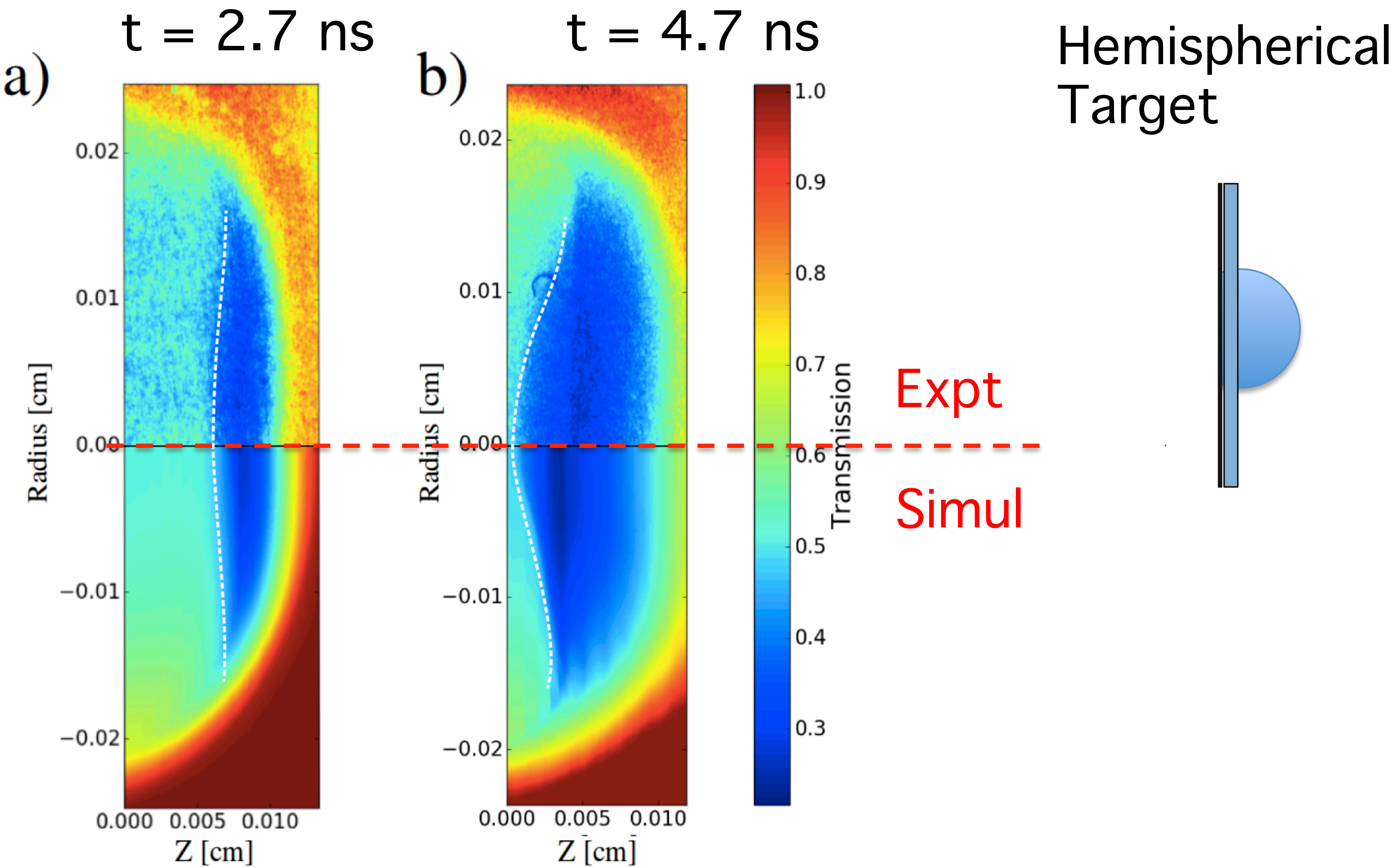

Synthetic radiographies

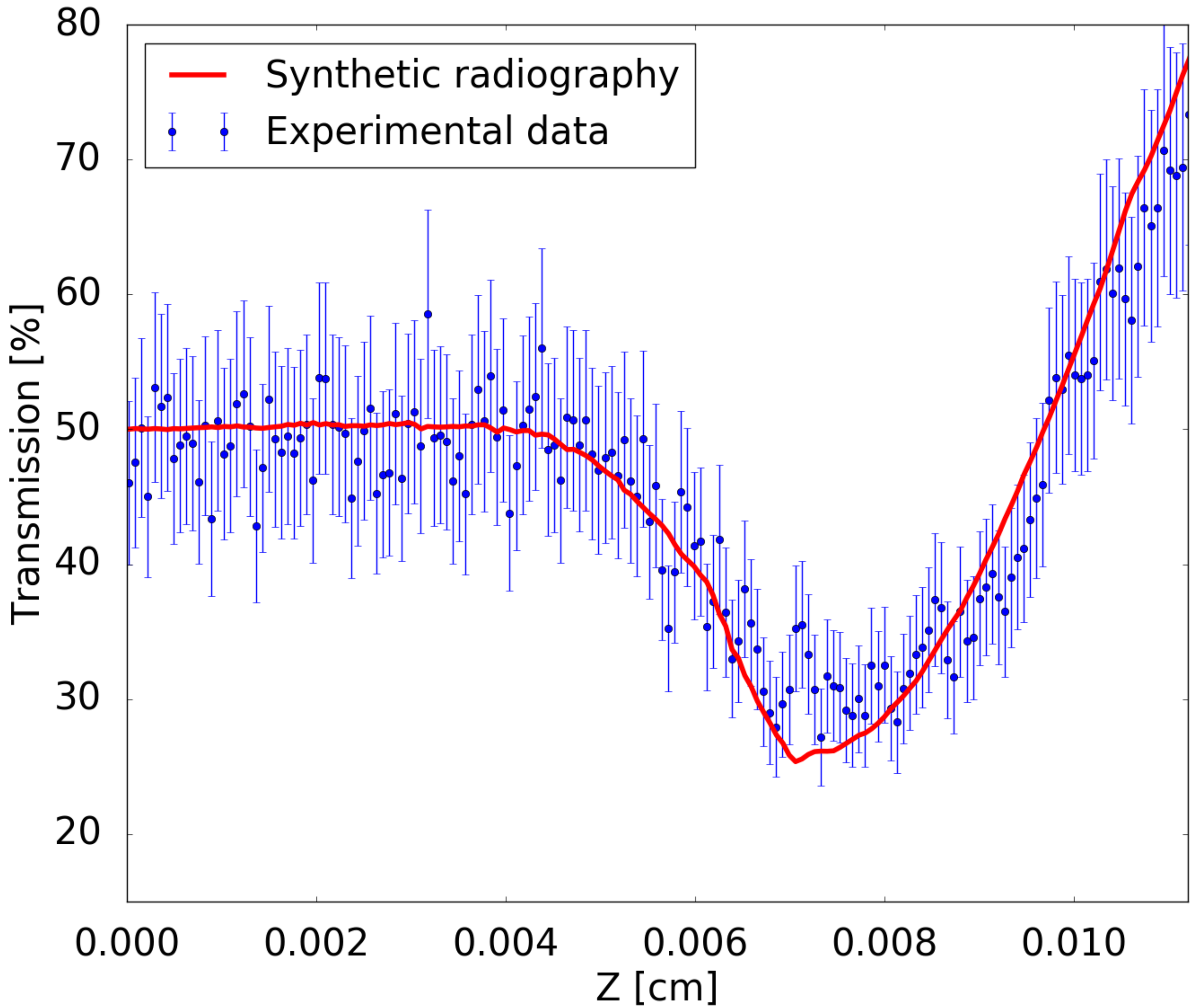

Comparison of measured / predicted transmission

$t = 2.7$ ns

1D radiography with ns beam

X ray radiography for time-resolved imaging of shock propagation

Laser GEKKO Osaka Univ

Shock produced inside Beryllium target (100 µm)

Ti foil used as X-ray backlighter

Image is time resolved by an X-ray streak camera couple to a pin-hole

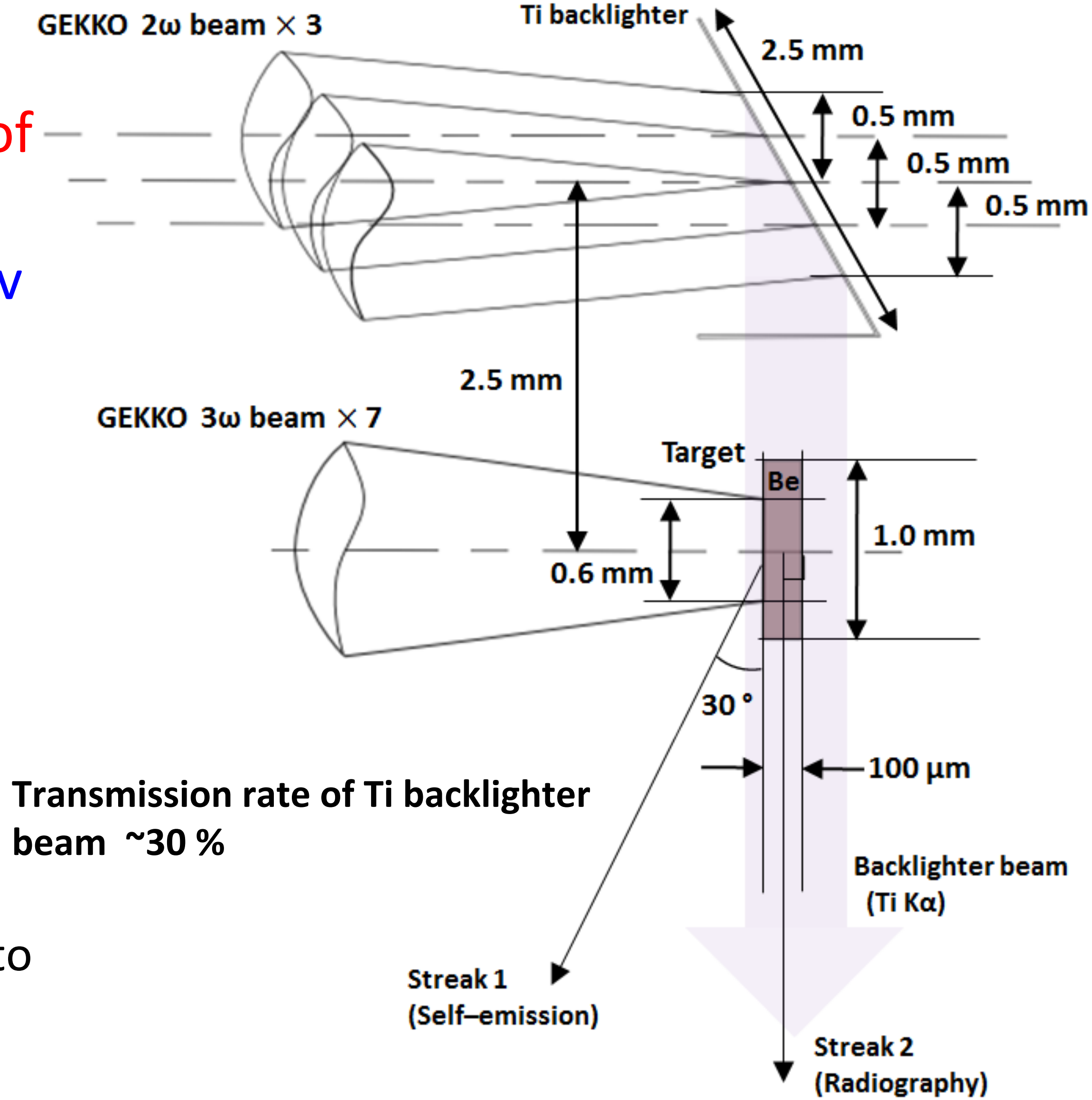

1D radiography with ns beam

Radiography image (raw)

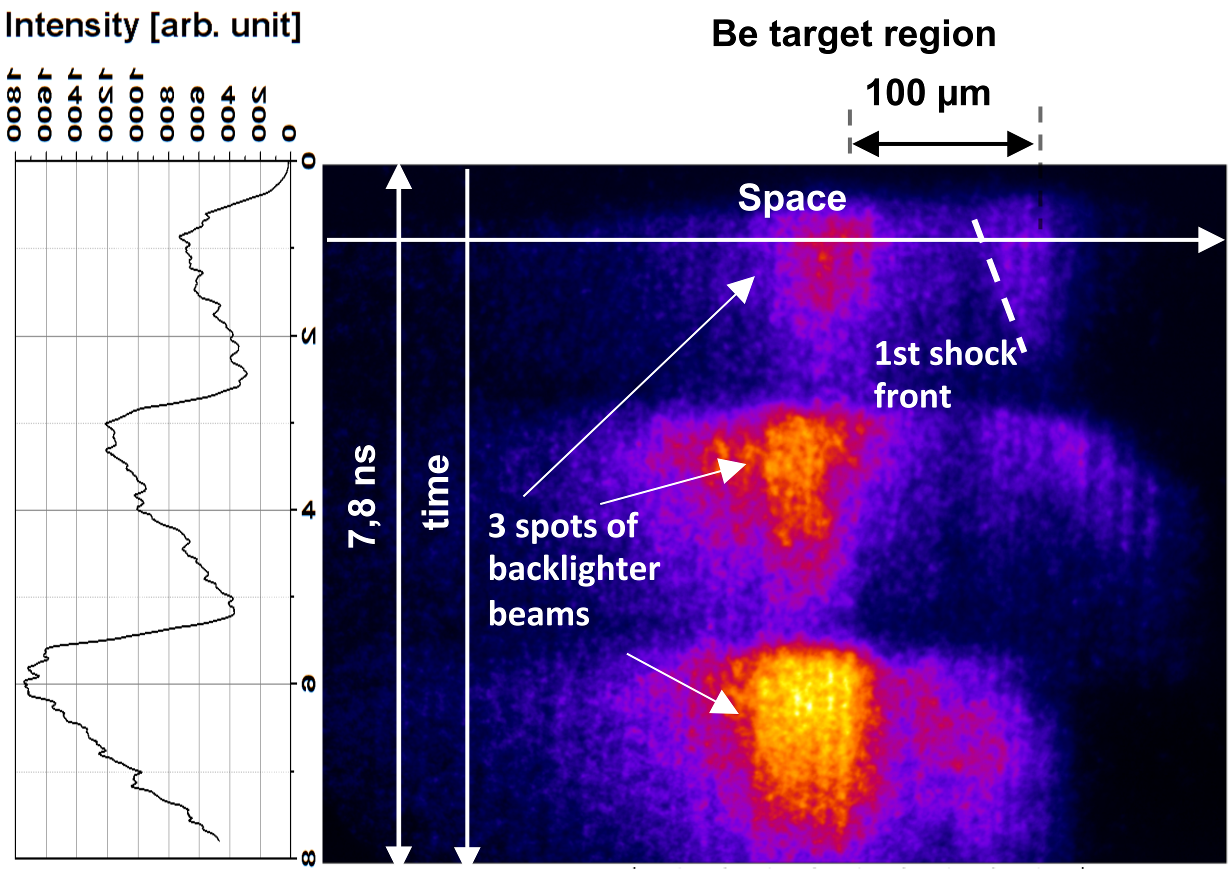

Spatial backlighter profile

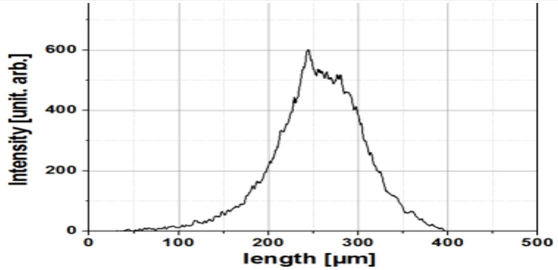

The knowledge of the spatial and temporal profiles of the X-ray backlighting source allow for image deconvolution

1D radiography with ns beam

The image is normalized using spatial and temporal profiles of backlighter emission.

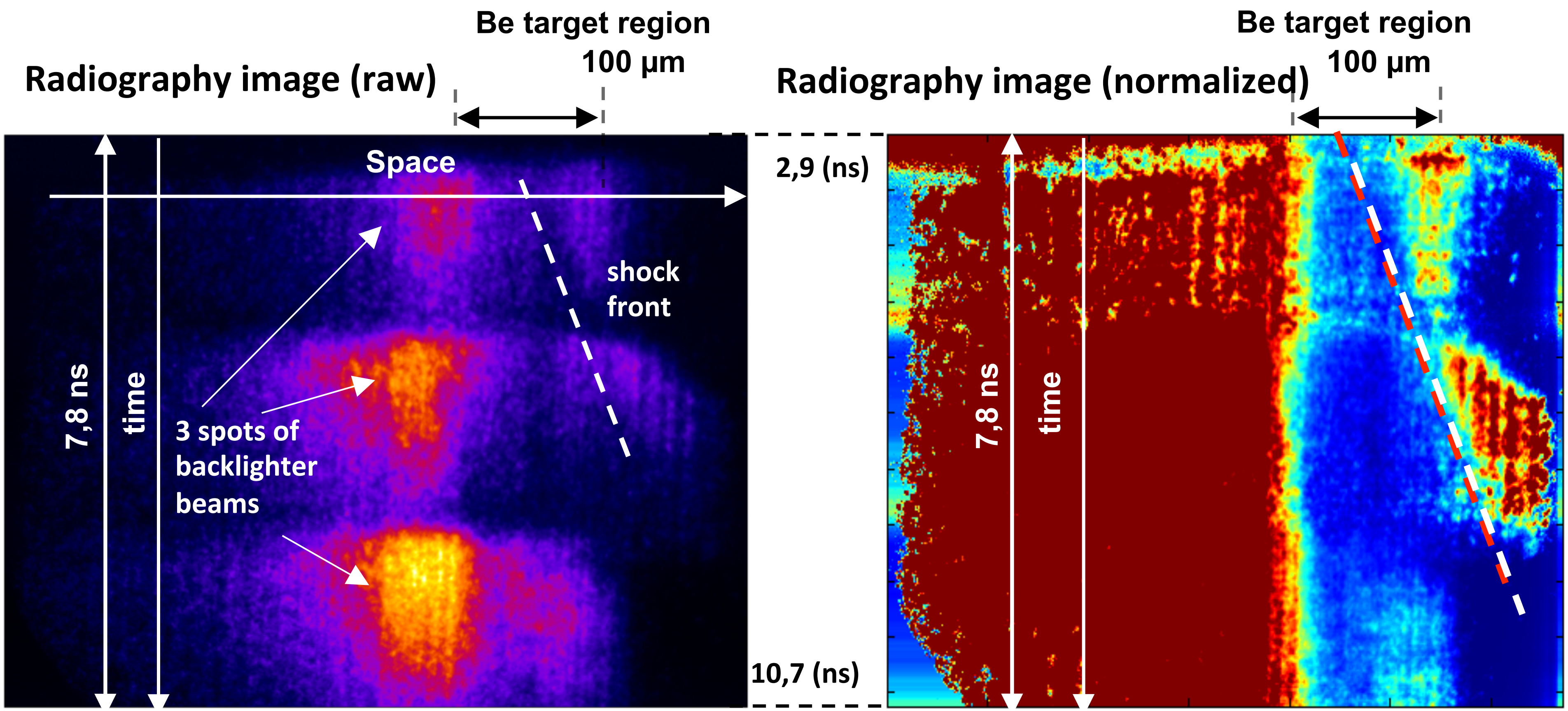

Average shock speed 19 km/s in agreement with hydro simulations

Experimental result vs simulation

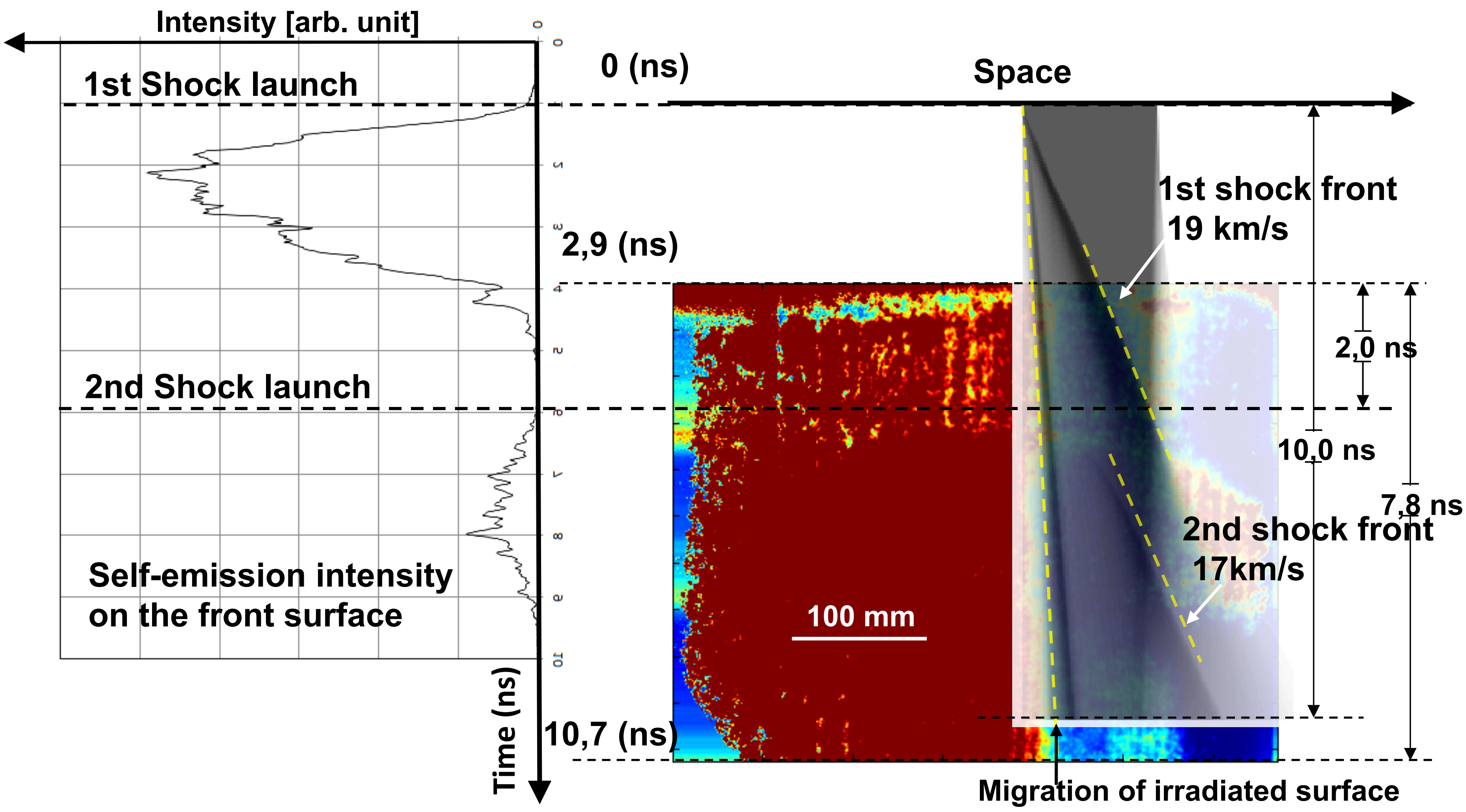

The code CHIC reproduces the hydrodynamics of this experience.

Conclusions

In order to understand the physics of Shock Ignition we require a variety of diagnostics

- **Concerning shock dynamics, SOP and VISAR allows reconstructing the chronometry and the velocity of the shock (i.e. to infer the pressure at any time)**

- **However they might be blinded by the intense preheating associated to Hot electrons / X-rays from the corona / strong shock precursor**

- **Radiography allow to follow shock dynamics and to measure compression. However care must be taken in the interpretation of radiographic images.**
  In any case it is difficult to evidence the presence of successive shocks following the first one

Many thanks to the main collaborators:

S.Baton (LULI, Ecole Polytechnique, France)

S.Atzeni, L.Antonelli (University of Rome "La Sapienza", Italy)

E.Lebel, Ph.Nicolai, A.Colaitis, V.Tikhonchuk (CELIA, Bordeaux, France)

E.Krousky, O.Renner (PALS, Prague, Czech Republic)

K.Shighemori (ILE, University of Osaka, Japan)

S.Brygoo, C.Rosseaux (CEA, Bruyeres, France)

Laser Megajoule

≥ 20% of shots will be allocated for civilian academic research oriented towards fusion for energy

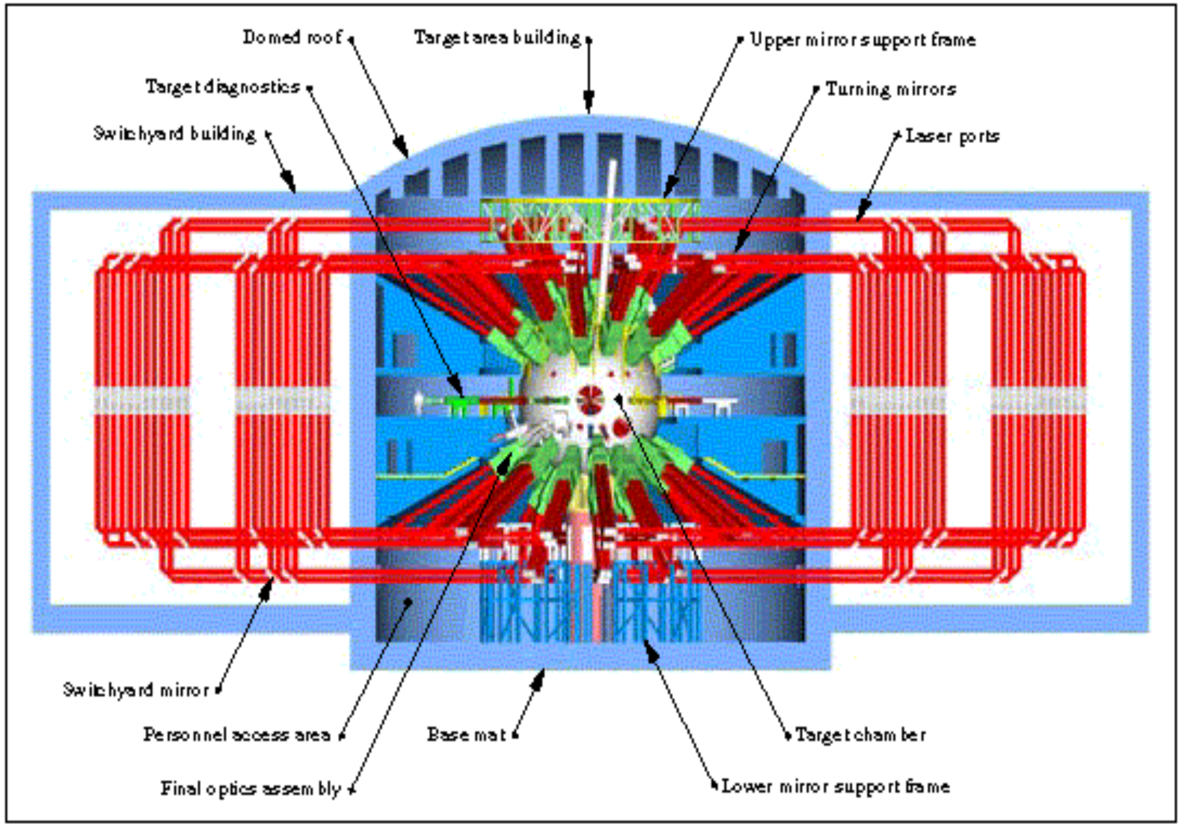

Nd:glass
2 MJ
10 ns
160 beams

Goal:
Performing shock ignition demonstration experiments

CELIA

Polar Direct Drive (PDD)

An example of how it can be done…

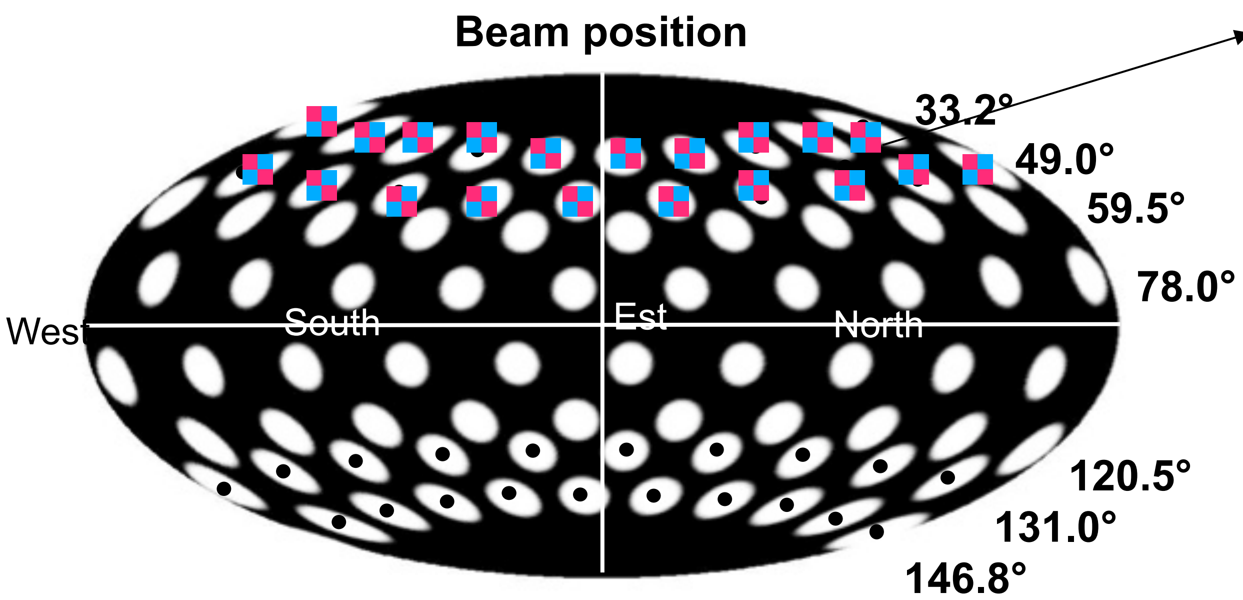

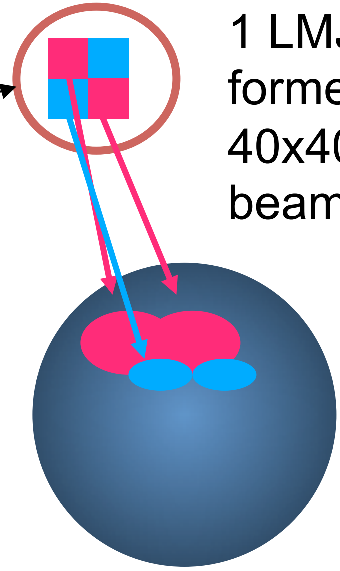

1 LMJ Quad formed from 4 40x40 (cm) beams

May be split and repointed on a sphere for optimal illumination

40 quads pattern : - uses quad splitting, defocusing and repointing (Polar Drive)

80 beams for compression + spike (PDD) 3.8 kJ,

80 beams for spike only (DD, tight focus) 0.75 kJ

"combined" approach: no beam is only used for compression

300 Mbar demonstrated on Omega

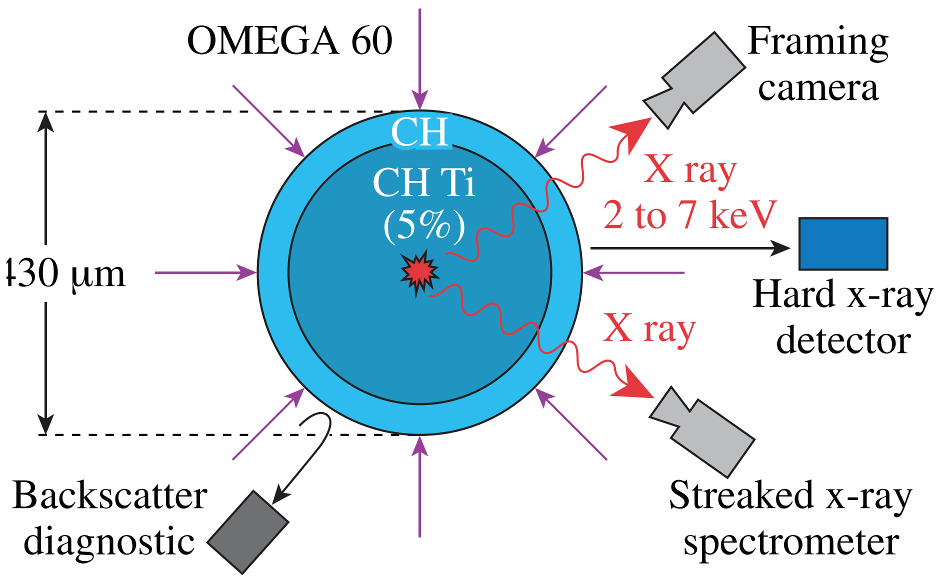

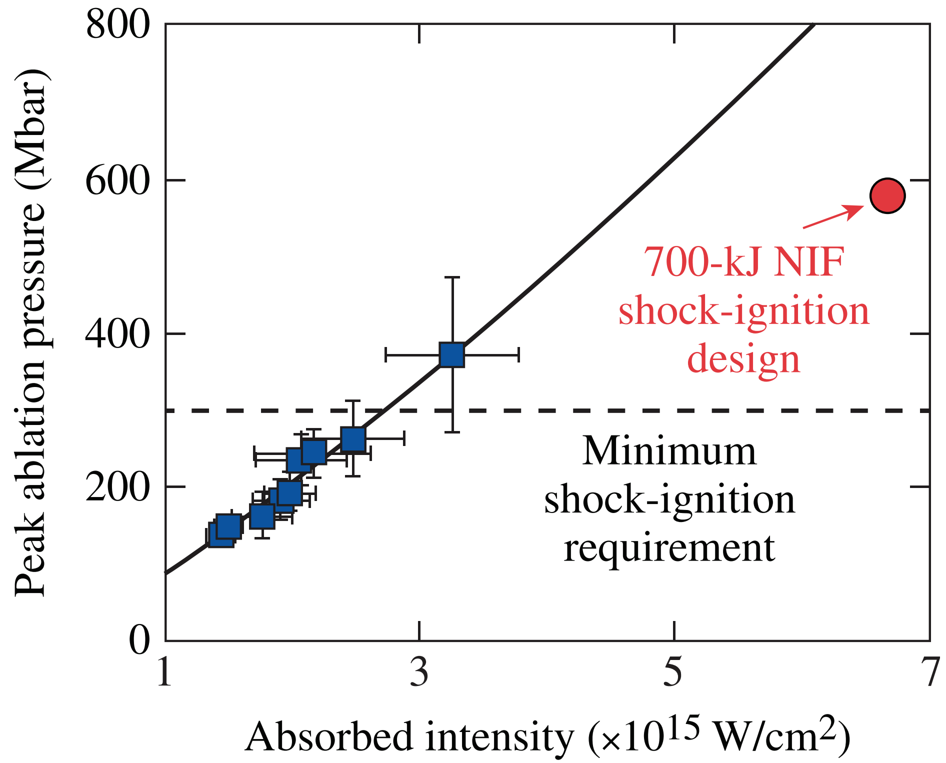

Difference between classical ablation pressure and hot electron driven pressure

isothermal corona: laser ablation

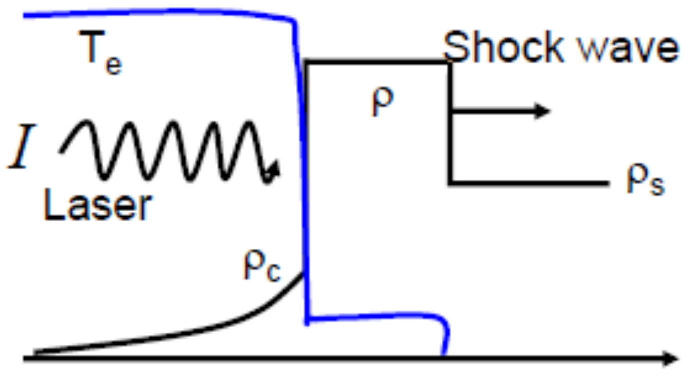

$$I = 4\rho_c C_s^3 \qquad C_s \propto T_e^{1/2}$$

$$P \propto \rho_c C_s^2 \qquad T_e \propto \left(\frac{I}{\rho_c}\right)^{2/3}$$

$$P \propto I^{2/3} \rho_c^{1/3}$$

ρ_c Critical density
(0.03 g/cc at 0.35 μm)

For extended corona: delocalised absorption, decrease of pressure

isothermal corona: hot electron ablation

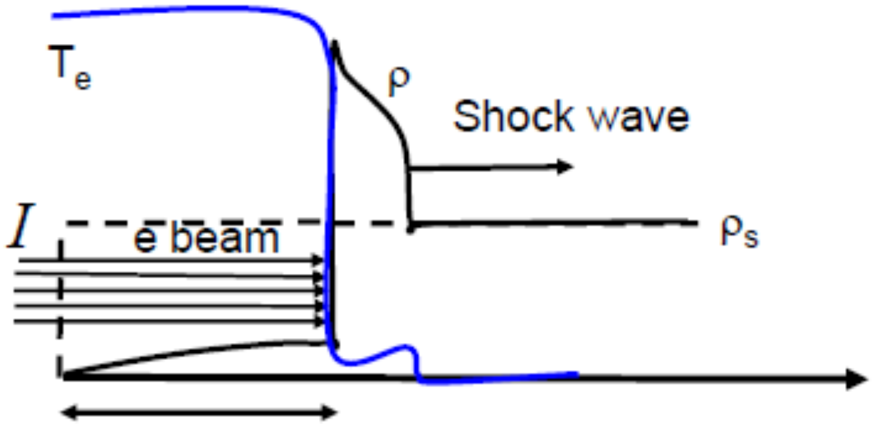

$\lambda_p = \chi_{he} / \rho_s$ Hot electron stoping lenght

Time to estabilsh pressure

$$t_s \propto \frac{\chi_{he}}{I^{1/3} \rho_s^{2/3}}$$

$$P \propto I^{2/3} \rho_s^{1/3}$$

ρ_s Solid density
(10 g/cc for SI DT)

The penetration depends only on the integrated ρr

Diagnostics in front side: Kα imaging

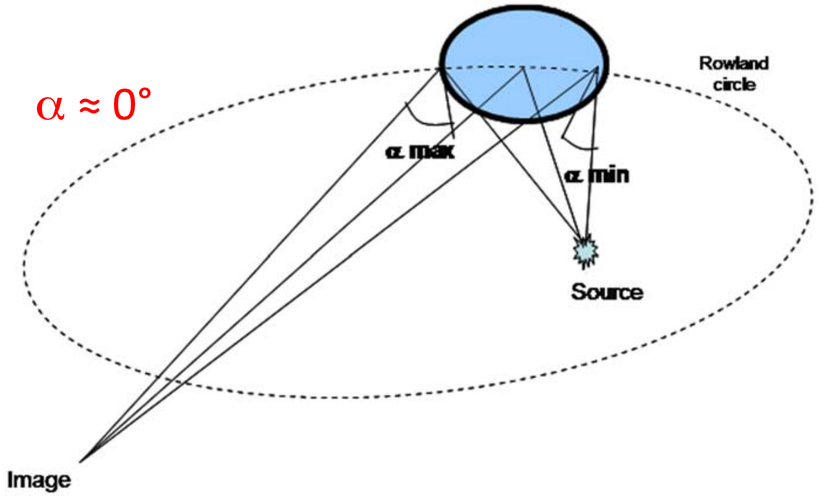

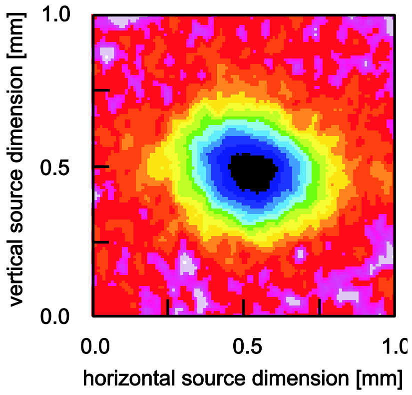

Kα spot: FWHM ≈ 200 μm (usually it is larger than focal spot, confirmed by MCPNX simulations)

Integration: total number of photons

Estimation of hot electron temperature from analysis of Kα signal vs. thickness of plastic overlayer ➔ Penetration ≈ 27 μm corresponding to electrons of energy between 30 and 50 keV (if monoenergetic)

From K-α to hot electrons
Conversion efficiency <1 %

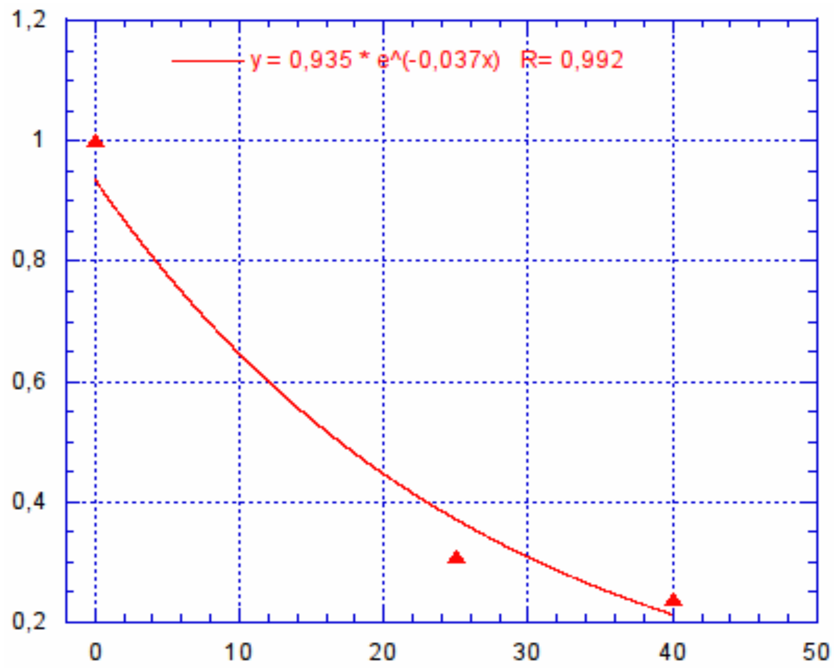

Diagnostics in front side: hot electrons

Estimation of hot electron temperature from ratio of Cu Kα to Ti Kα

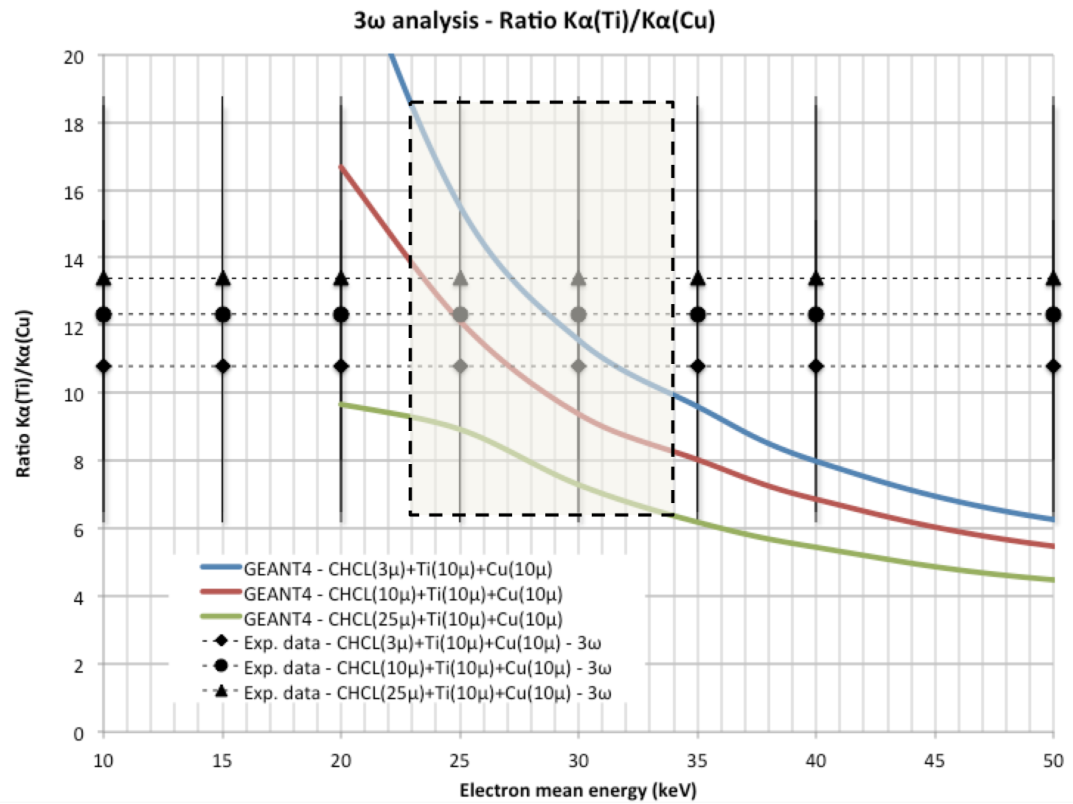

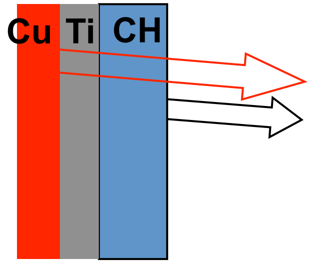

Hot electrons:
Kα of Cu
Kα of Ti

Hot electrons

Estimated from

- **X-ray photon counting**
- **Kα images and spectroscopy**

T_h ~ 28.5±4.5 keV,
0.65±0.30 % conversion,
≈ 3 10^{14} electrons

Diagnostics in front side: backscattering

Impact of parametric instabilities

SRS spectra vs. delay

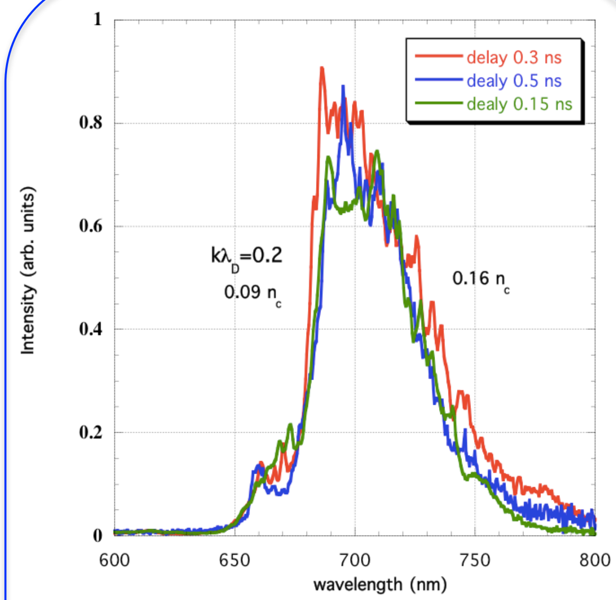

⇒ **densities between 9% and 16% n_c**

Correlation between Raman signal and Kα photon number

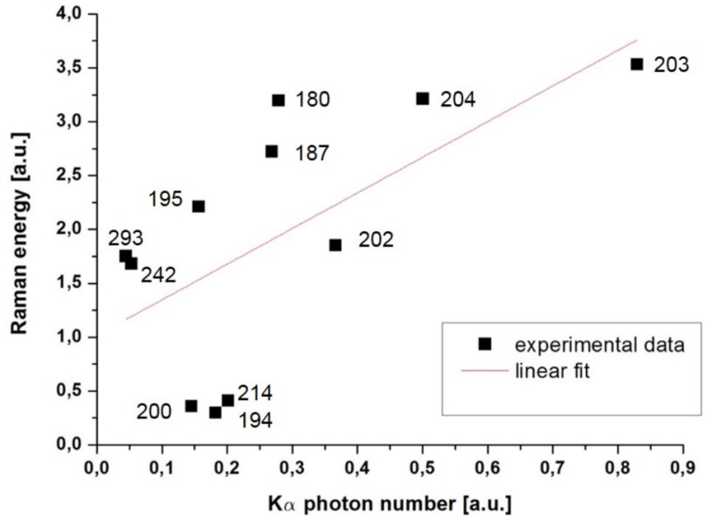

➢**Reflectivity mainly dominated by SBS**

LIL: backscattering

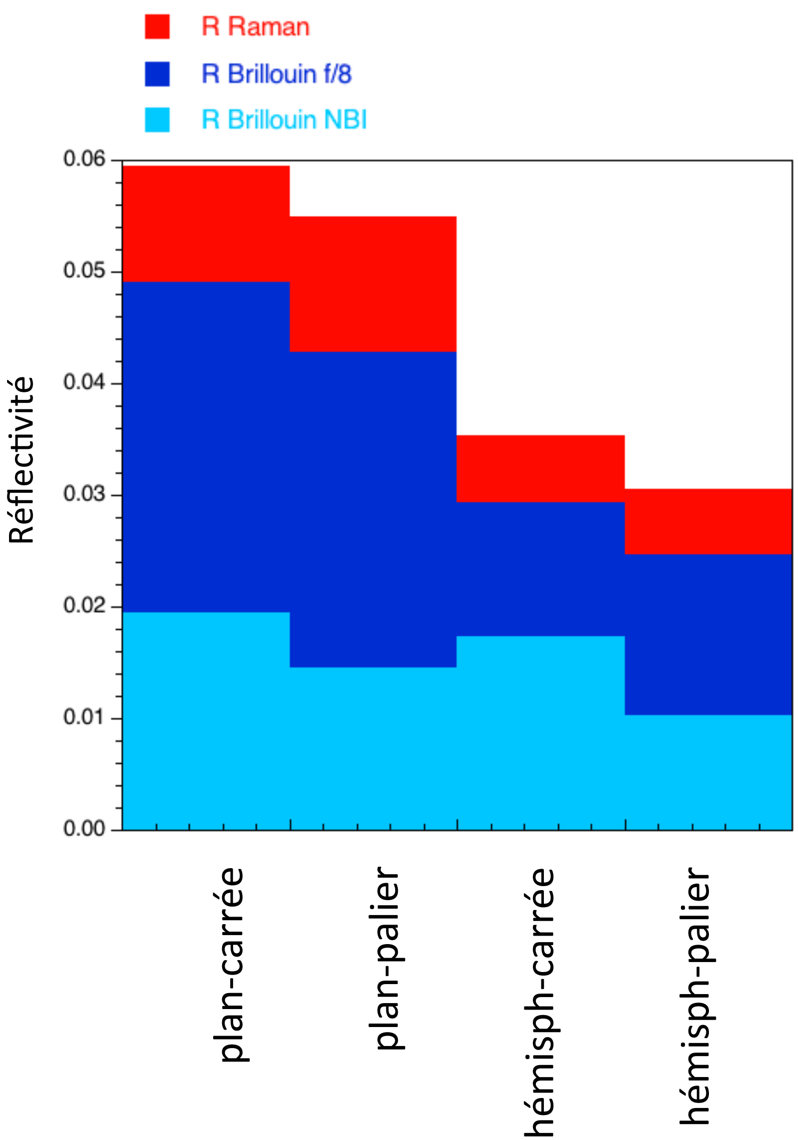

First conclusions:

- Low Backscattering:
≤ 5% of total laser energy
≤ 8% of energy within Ø500 µm spot.

- Less energy backscattered with spherical targets (a factor of 2*x* in total, with NBI) and of 3*x* within the lens cone (f/8).

- Little differences with or without preplasma

- ≈1/3 SRS and 2/3 SBS within f/8, i.e. typically ≤ 3% SBS and ≤ 1.5% SRS (no SRS measurement by the NBI and about 1.5-2% of SBS out of the lens cone)